LA-11222-MS

Preliminary Survey of the Stability of Silica-Rich Cementitious Mortars 82-22 and 84-12 with Tuff

Los Alamos

Los Alamos National Laboratory is operated by the University of California for the United States Department of Energy under contract W-7405-ENG-36.

This work was supported by the Yucca Mountain Project Office as part of the Civilian Radioactive Waste Management Program. This Project is managed by the US Department of Energy, Nevada Operations Office.

An Affirmative Action/Equal Opportunity Employer

LA-11222-MS

UC-70
Issued: March 1989

LA--11222-MS

DE89 009692

Preliminary Survey of the Stability of Silica-Rich Cementitious Mortars 82-22 and 84-12 with Tuff

*Barry E. Scheetz**
*Della M. Roy**

**Consultants at Los Alamos. Materials Research Laboratory, Pennsylvania State University, University Park, PA 16802.*

Los Alamos National Laboratory
Los Alamos, New Mexico 87545

Contents

PRELIMINARY SURVEY OF THE STABILITY OF SILICA-RICH CEMENTITIOUS MORTARS 82-22 AND 84-12 WITH TUFF

by

Barry E. Scheetz and Della M. Roy

ABSTRACT

Two cementitious formulations were prepared that contained mixtures of silica-adjusted cementitious binder and tuff of the Topopah Spring Member. Both formulations were developed to possess a bulk chemical composition that approached the bulk silica-to-alumina ratio of the tuff of the Topopah Spring Member. The two formulations represent examples of an expansive (82-22) and a nonexpansive (84-12) cementitious sealing material. The expansive grout relies on the the formation of ettringite to generate the expansive forces.

Phase characterization of the reaction products for the expansive grout revealed that the expansive agent, ettringite, was not stable above about 100°C. Tobermorite was observed at all temperatures, even at 300°C, well above its expected stability limit. The incorporation of Al into the tobermorite structure is postulated as contributing to the enhanced thermal stability. In the longer experiments, at 200 and 300°C, the Al-tobermorite partially reacted with excess SiO_2 to form truscottite, another calcium silicate hydrate. This observation is consistent with the solution analyses that suggest that the liquid phase in contact with the seal material is very nearly at equilibrium with respect to quartz at 150°C and slightly undersaturated with respect to quartz at 200°C.

1. INTRODUCTION

The design of cementitious materials for sealing a nuclear waste repository in a geological environment must address the question of performance: how this "man-made" material in contact with the host rock affects the repository's ability to isolate wastes from the biosphere. One of the many properties that affect repository performance is chemical reactivity, the subject of this report.

One aim of any designed cementitious sealing material is to minimize or eliminate any chemical potential gradients and prevent destabilization of the sealing system.

Compatibility of the host rock with respect to concrete can be approached in two ways. First, sands and aggregates derived from the host rock can be used in the concrete formulations. The assumption in this approach is that the bulk of the sealing material is composed of rock similar to the rock of the emplacement environment. Therefore, the chemistries of the host tuff and concrete should be similar, with only a minor perturbation caused by the relatively small amount of cement in the concrete (20 to 30%). Our first experimental study examined this concept through an investigation of the reactivity of a tuff-bearing concrete, CL-40 CON-14, using a partly modified cement composition, local Nevada Test Site (NTS) concrete sand, and coarse aggregates made from the Grouse Canyon Member of the Belted Range Tuff. The results of this study are presented in Scheetz and Roy (in preparation).

The second approach to design of compatible cementitious sealing materials is to control the bulk chemical composition of the sealing material so that it approaches the bulk chemical composition of the geologic host. This approach seeks chemical compatibility between the components of the seal material and the host rock. Because of the high-silica content of the Yucca Mountain tuffs, concretes with a cementitious matrix having high-silica content are likely to be more compatible with the tuff than are normal portland cement concretes with high calcium content matrices.

This latter approach was followed in the design of the two grouts that were evaluated in this study. The design of the sealing material was initially based upon the use of a commercially available shrinkage-compensating cement, which in turn was modified with reactive silica-rich admixtures. The bulk chemistry of the grouts was carefully chosen to provide for the maximum formation of cementitious phases by reaction between the cementitious matrix and an aggregate that was a constituent of the host rock. The expansive agent in the commercial cement is ettringite, which is formed during hydration by the reaction of a soluble calcium sulfate source and a source of calcium aluminate. An alternative formulation was developed that closely approximated the shrinkage-compensated mixture in bulk chemistry but did not contain the calcium sulfate source. This latter low-sulfate formulation was evaluated in an effort to minimize the release of sulfate to the groundwater.

2. EXPERIMENTAL

2.1 Methods

Most of the experimental methods used, including the equipment for elevated temperature (and pressure) reaction studies, and the characterization and test methodology have been described in a previous report (Scheetz and Roy, in preparation). Below are described the characteristics of the materials used in the current tests and the specific test designs.

2.2 Materials Characterization

2.2.1 Grout Formulations

The grouts used in this stability-testing program are schematically represented in Fig. 1a and b. The shrinkage-compensated formulation, 82-22, represented in Fig. 1a is composed of approximately equal masses of sand, cement, and all other admixtures including water. The total cementitious solids make up about 50% of the mass of the formulation.

The low-sulfate 84-12 formulation represented in Fig. 1b contains a conventional Class H cement plus slag and reactive-silica admixtures. The combined cementitious solids in this formulation amount to 56% of the total mass. Tables I and II represent the grout formulation in terms of oxide composition, with and without the sand.

2.2.2 Cement

The cement (Z-47) used in the 82-22 grout formulation is a shrinkage-compensated cement. It is designed to develop expansion based on the formation of ettringite during the early stages of hydration. A standard coarse-grind oil-well cement (H-10) was chosen for the 84-12 formulation. The bulk chemical analysis is presented in Table III.

2.2.3 Fly Ash

The fly ash used in this formulation is a representative of a class of fly ash derived from eastern bituminous coals, ASTM Class F. The mineralogical composition of this ash is dominantly quartz, mullite, and iron oxide (Scheetz et al., 1982). In addition, a major portion of the fly ash is an x-ray-amorphous glassy phase having its major amorphous band maximum at <3.7Å, suggesting a silica-rich silicate glass. The chemical reaction

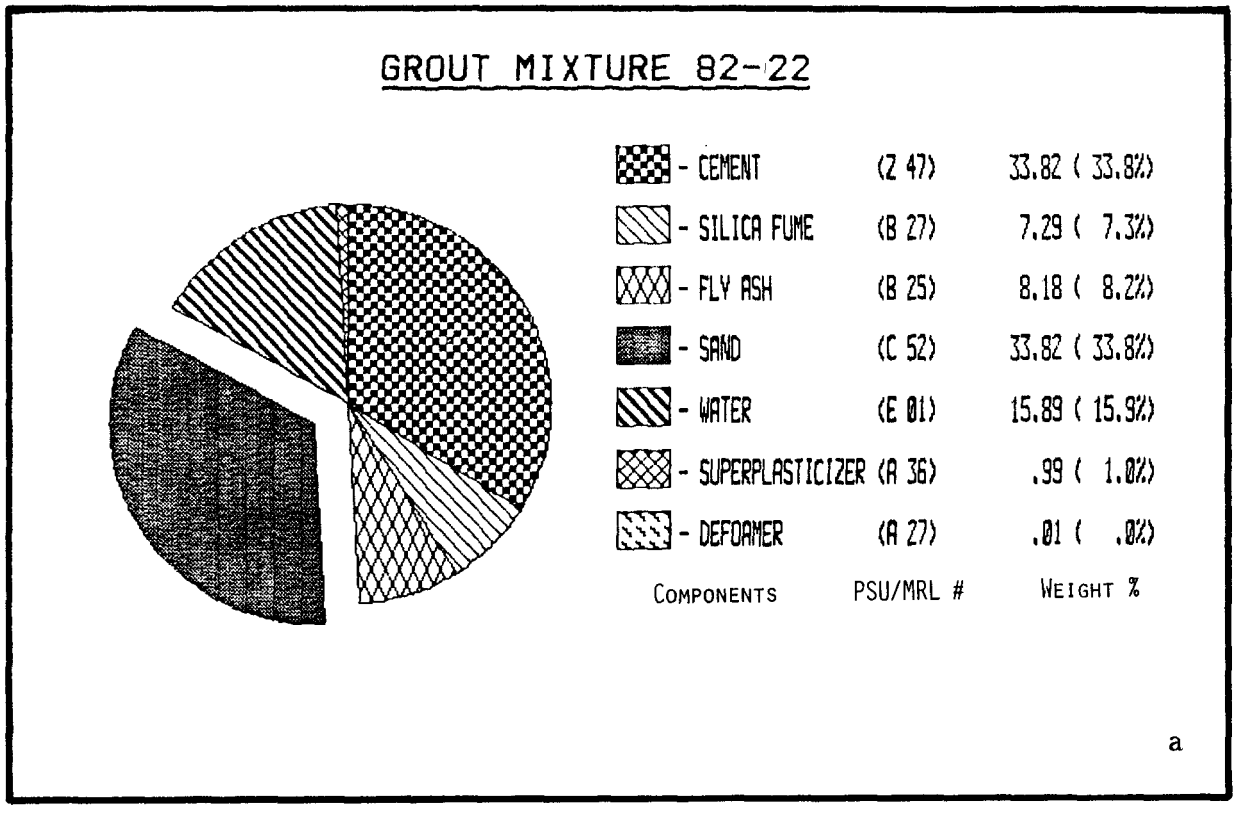

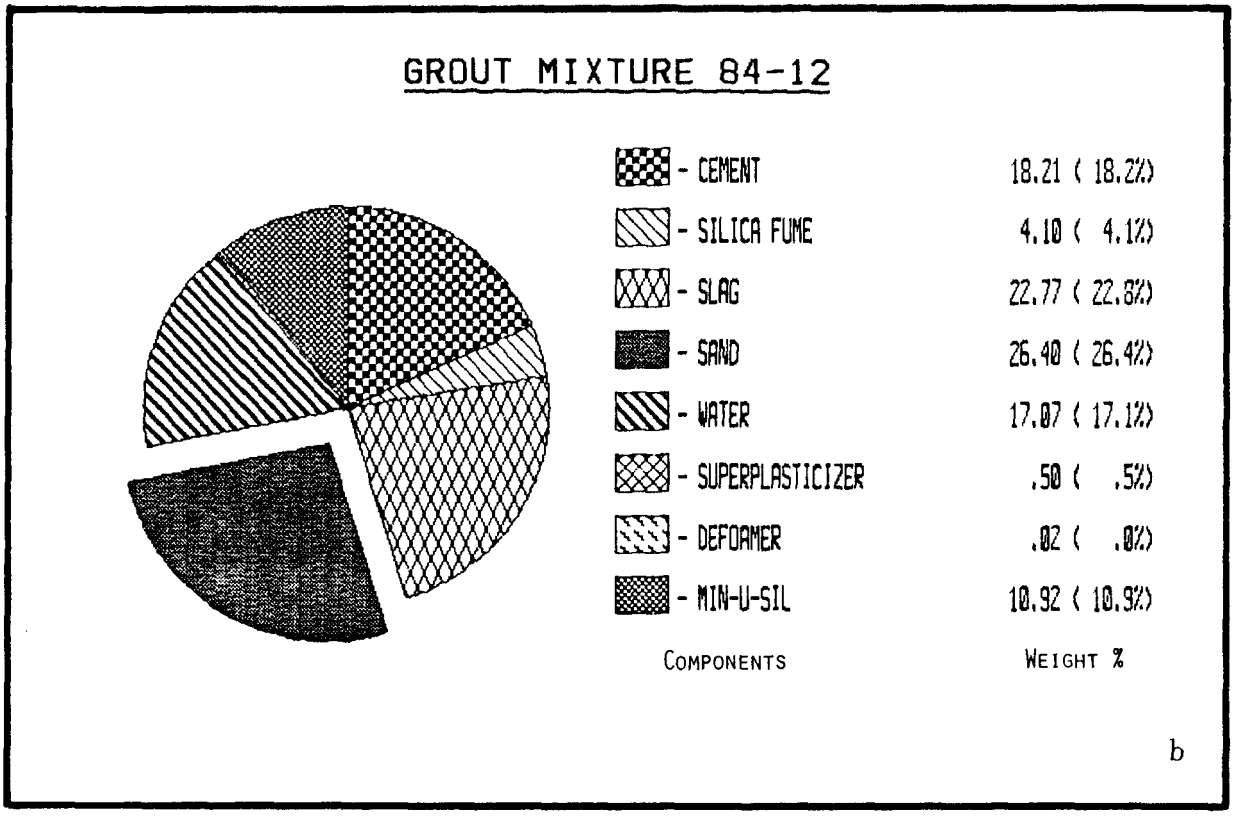

Fig. 1. Schematic representation of (a) 82-22 mortar and (b) 84-12 grout compositions.

TABLE I

BULK CHEMICAL COMPOSITION OF GROUTS

	Grout (wt %)	
Oxide	82-22	84-12
SiO_2	64.16	61.98
Al_2O_3	4.50	4.19
Fe_2O_3	2.74	1.10
CaO	25.88	27.52
MgO	1.83	4.65
MnO	0.12	0.17
Na_2O	0.10	0.10
K_2O	0.48	0.27
P_2O_5	0.11	0.02
Total	99.92	100.00

TABLE II

BULK CHEMICAL COMPOSITIONS OF GROUTS WITHOUT SAND AGGREGATE

	Grout (wt %)	
Oxide	82-22	84-12
SiO_2	38.60	48.45
Al_2O_3	7.74	5.44
Fe_2O_3	4.72	1.59
CaO	44.59	37.69
MgO	3.14	6.05
MnO	0.04	0.22
Na_2O	0.15	0.13
K_2O	0.83	0.40
P_2O_5	0.18	0.04
Total	99.99	100.01

TABLE III

CHEMICAL ANALYSIS OF

THE SHRINKAGE-COMPENSATED AND CLASS H CEMENTS

	Weight %	
Oxide	Z-47	H-10
SiO_2	20.1	22.24
Al_2O_3	4.11	3.58
TiO_2	0.22	0.18
Fe_2O_3	3.19	3.94
MgO	4.18	3.87
CaO	62.26	62.99
MnO	0.048	0.022
SrO	0.05	0.06
BaO	0.05	0.02
Na_2O	0.14	0.13
K_2O	0.45	0.53
P_2O_5	0.12	0.08
SO_3	4.59	1.92
L.O.I.[a] (1000°C)	2.04	0.66
Total	101.45	100.22

[a]Loss on ignition.

rate of this fly ash is slow because of the insoluble crystalline phases and slowly reacting glass composition. Its function in the mortar formulation is to provide additional sources of both alumina and silica that will be released at a somewhat slower rate than the highly reactive silica fume. The bulk chemical composition of the fly ash is presented in Table IV.

2.2.4 Silica Fume

This form of x-ray-amorphous silica is produced as an industrial by-product from the reduction of silica sand to silicon metal. It results from the oxidation of silicon vapors above the hearth. The particle size of the fume samples is typically submicrometer. The

small particle size coupled with the amorphous nature makes silica fume a very reactive admixture in cementitious environments. The bulk chemical composition of the fume is presented in Table IV.

TABLE IV

CHEMICAL COMPOSITION OF

FLY ASH (B25), SILICA FUME (B27), AND SLAG (B66)

	Weight %		
Oxide	Fly Ash	Silica Fume	Slag
SiO_2	50.2	96.0	34.3
Al_2O_3	27.0	0.10	10.2
TiO_2	1.40	<0.1	0.48
Fe_2O_3	13.8	<0.1	0.67
MgO	0.84	0.13	11.4
CaO	1.82	0.12	40.61
MnO	0.034	0.010	0.51
Na_2O	0.24	0.1	0.19
K_2O	2.45	0.45	0.45
P_2O_5	0.49	0.07	0.02
SrO			0.05
BaO			0.05
S			1.31
Total	98.27	96.86	100.24

2.2.5 Slag

The granulated blast-furnace slag used is a calcium magnesium aluminosilicate glass, a by-product of the manufacture of steel, produced by the reaction of limestone with the gangue of the iron ore. The bulk chemical composition of the slag is more siliceous than portland cement. The granulated slag is largely glassy and metastable and therefore chemically reactive. Table IV summarizes the chemical composition of this slag.

2.2.6 Tuff Materials

A sample of tuff of the Topopah Spring Member, collected at Fran Ridge, was received from Los Alamos National Laboratory (LANL). A set of prism samples was cut with a water-cooled diamond saw from a block of this tuff [Pensylvania State University (PSU)/Materials Research Laboratory (MRL) #C58] for use as monoliths in the accelerated stability studies. The samples from Sandia National Laboratories (SNL) (PSU/MRL #C48 and C48Y Grouse Canyon Member, Belted Range Tuff) were mechanically crushed and sieved, and the -20+30 mesh sieve (840- to 590-μm) fraction was utilized in the rocking-autoclave studies.

2.2.6.1 Chemical Analysis

All three samples were analyzed for bulk chemical composition. The three samples possessed approximately the same composition with minor differences in iron and total alkalies. Analyses are given in Table V.

2.2.6.2 The XRD Characterization

The bulk x-ray diffraction (XRD) characterization of the three tuff samples indicated that the sample #C48 (from G-tunnel) was a zeolitized tuff, while samples #C48Y (also from G-tunnel) and #C58 (from Fran Ridge, Topopah Spring Member) were nonzeolitized tuffs. All tuff samples contained cristobalite and two feldspars, a K-feldspar and a plagioclase. The closest match of the specimens to Joint Committee on Powder Diffraction Standards File (JCPDSF) reference patterns is presented in the summary of identified phases in Table VI.

2.2.6.3 Petrographic Characterization

Thin sections of each tuff were observed with crossed nicols and in plane-polarized light to observe rock textures and mineralogy. The groundmass of sample #C48 was largely amorphous, reddish-brown, and more or less opaque to transmitted light, enclosing lithic fragments, feldspar crystals, and some glass shards. There was evidence of devitrification in bands and zones of fine intergrowths of silica phases and fibrous feldspars, which are visible in crossed-polarized light.

Samples #C48Y and #C58 were much lighter colored in plane-polarized light, with far more extensive recrystallization of groundmass. Both were densely welded,

TABLE V

CHEMICAL ANALYSIS OF TUFF SAMPLES

	Weight %		
	Grouse Canyon		Topopah Spring
Oxide	C48	C48Y	C58
SiO_2	75.04	73.6	75.4
Al_2O_3	10.0	11.3	12.1
TiO_2	0.28	0.28	0.10
Fe_2O_3	2.71	3.09	0.90
MgO	0.20	0.15	0.14
CaO	0.32	0.25	0.43
MnO	0.105	0.133	0.059
Na_2O	2.13	3.39	3.86
K_2O	6.74	5.95	4.98
P_2O_5	0.09	0.03	0.06
SO_3	0.03	<0.1	<0.1
L.O.I.[a] 950°C	1.67	1.3	1.4
Total	99.32	99.58	99.43

[a]Loss on ignition.

with deformation and alignment of pumice fragments and glass shards. More complete characterization of a variety of samples from the Topopah Spring Member is given in Broxton et al. (1982).

2.2.7 J-13 Groundwater

Five 2-ℓ containers of groundwater from J-13 wells were provided to MRL by Los Alamos for use as the fluid in the reaction experiments. These samples were individually analyzed and are reported in Table VII.

2.3 Simulated Concretes

Figure 2a and b summarizes the compositions of the simulated concretes utilized in these experiments. In all of the agitated experiments a mechanical mixture of -20+30

TABLE VI

SUMMARY OF PHASE COMPOSITION OF TUFF SAMPLES AS DETERMINED BY XRD

Phase	JCPDSF #	C48	C48Y	C58
Quartz	5-4901	?	?	x
Cristobalite[a]	11-695	x	x	x
Sanidine	19-1127	x	x	x
Oligoclase	20-548	?	x	x
Illite[b]	9-343	-	-	x
Heulandite[c]	25-144	x	-	-

[a]Plus tridymite in C48Y and C58.

[b]Possibly mica.

[c]Possibly clinoptilolite.

sieve size (590- to 840-μm diam) powders of tuff and hardened grout in the proportions of 2 parts tuff to 1 part grout were used. Figure 3 is a CaO-Al_2O_3-SiO_2 ternary diagram showing the composition of the cementitious formulations and tuff of the Topopah Spring Member.

2.4. Experimental Design

Experiments were performed using high surface area powders to increase the rate of possible reaction between the tuff and the cementitious matrix. Agitation was also used in some of the fine-powder experiments to increase reaction rates. Monolithic samples made by slabbing cast specimens were also used to restrict reaction to the surfaces so that early-stage reactions between tuff and cementitious matrix could be examined. Most experiments were conducted at 200°C, which is anticipated to be higher than the upper temperature limit for a repository in tuff. Such temperatures could be reached in grout and concrete sealing canister emplacement holes. Table VIII summarizes the different materials and conditions of the tests.

TABLE VII

CHEMICAL ANALYSES OF J-13 GROUNDWATERS

	Bottle							
Element[a]	#1		#2	#3		#4		#5	
Al	<0.02		0.02	<0.02	(<0.2)	<0.2	(<0.2)	<0.02	(<0.2)
Ba	<0.02		<0.02	<0.02	--	<0.02	--	<0.02	--
Ca	15.5		15.9	15.9	(12.0)	16.3	(12.4)	15.9	(12.4)
Fe	<0.02		<0.02	<0.02	(<0.02)	<0.02	(<0.2)	<0.02	(0.3)
F	2.2		2.1	2.1	--	1.8	--	1.9	--
K	5.2		5.1	5.2	(9.5)	5.3	(9.0)	5.2	(6.8)
Li	0.06		0.06	0.05	--	0.05	--	0.05	--
Mg	1.96		1.93	1.99	(2.10)	1.98	(2.1)	1.97	(2.2)
Mn	<0.02		<0.02	<0.02	(<0.02)	<0.02	(<0.02)	<0.02	(<0.02)
Na	37.		37.	37.	(39.)	36.	(41.)	37.	(40.)
P	<0.05		<0.05	<0.05	(<0.2)	<0.05	(<0.2)	<0.05	(<0.2)
Si	33.		32.	32.	(26.)	32.	(28.)	32.	(28.)
SO_4	21.		19.	23.	--	21.	--	21.	--
Sr	0.04		0.04	0.04	--	0.04	--	0.04	--
Ti	<0.02		<0.02	<0.02	(<0.2)	<0.02	(<0.2)	<0.02	(<0.2)
V	<0.02		<0.02	<0.02	(<0.2)	<0.02	(<0.2)	<0.02	(<0.2)
ΣC	48.7	(63.7)[b]							
ΣOrganic C	14.3	(20.9)							
$CO_3^=$	43.0	(53.5)							
pH	7.7				(7.7)		(8.13)		(7.93)

[a] Concentrations expressed as mg/ℓ (ppm).

[b] Number in () represents replicate.

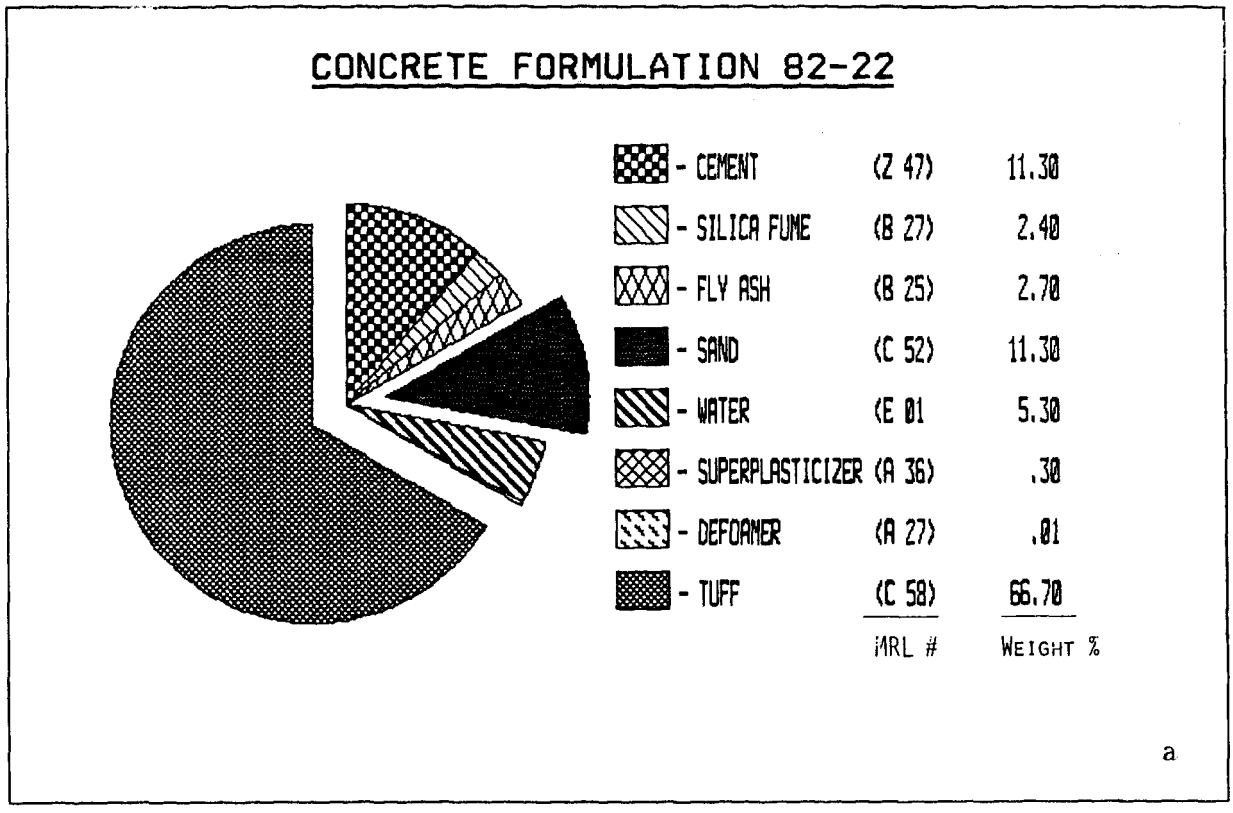

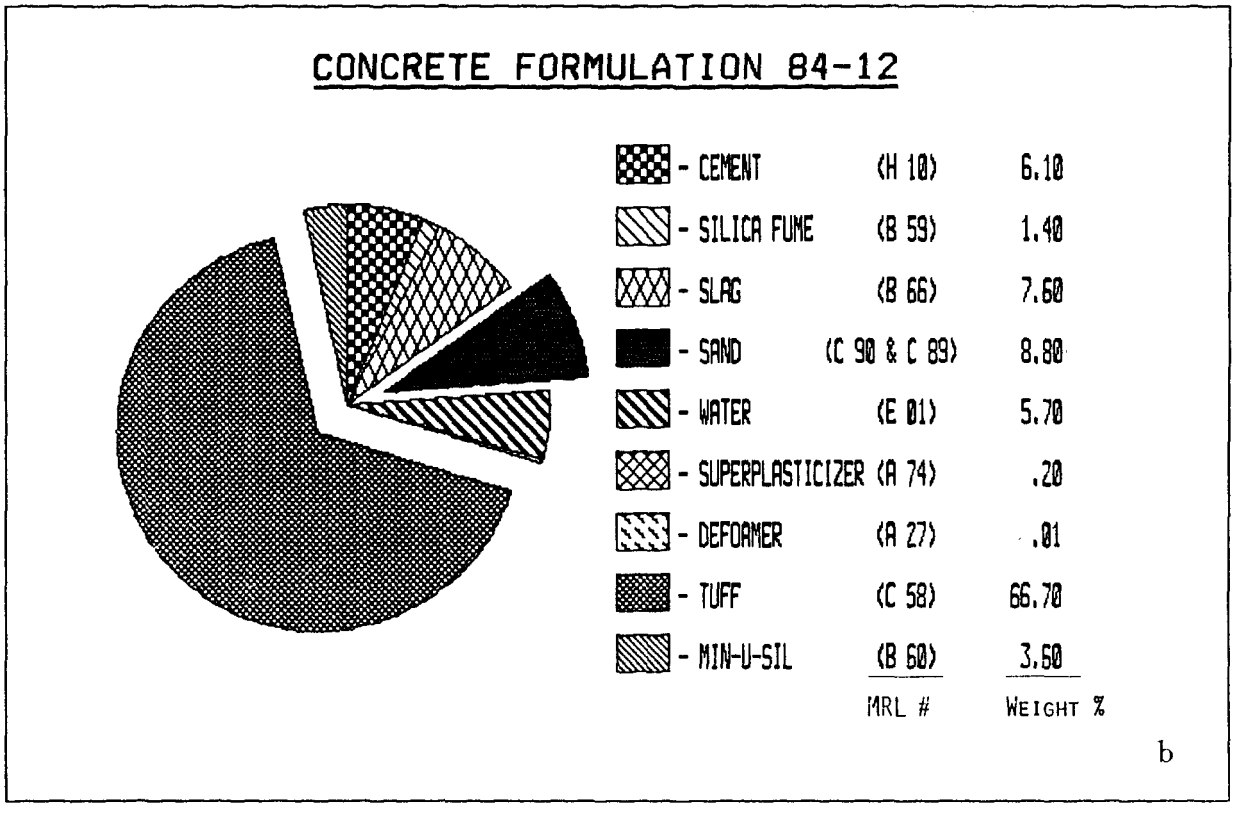

Fig. 2. Schematic representation of "artificial" concrete formulation based upon (a) 82-22 and (b) 84-12.

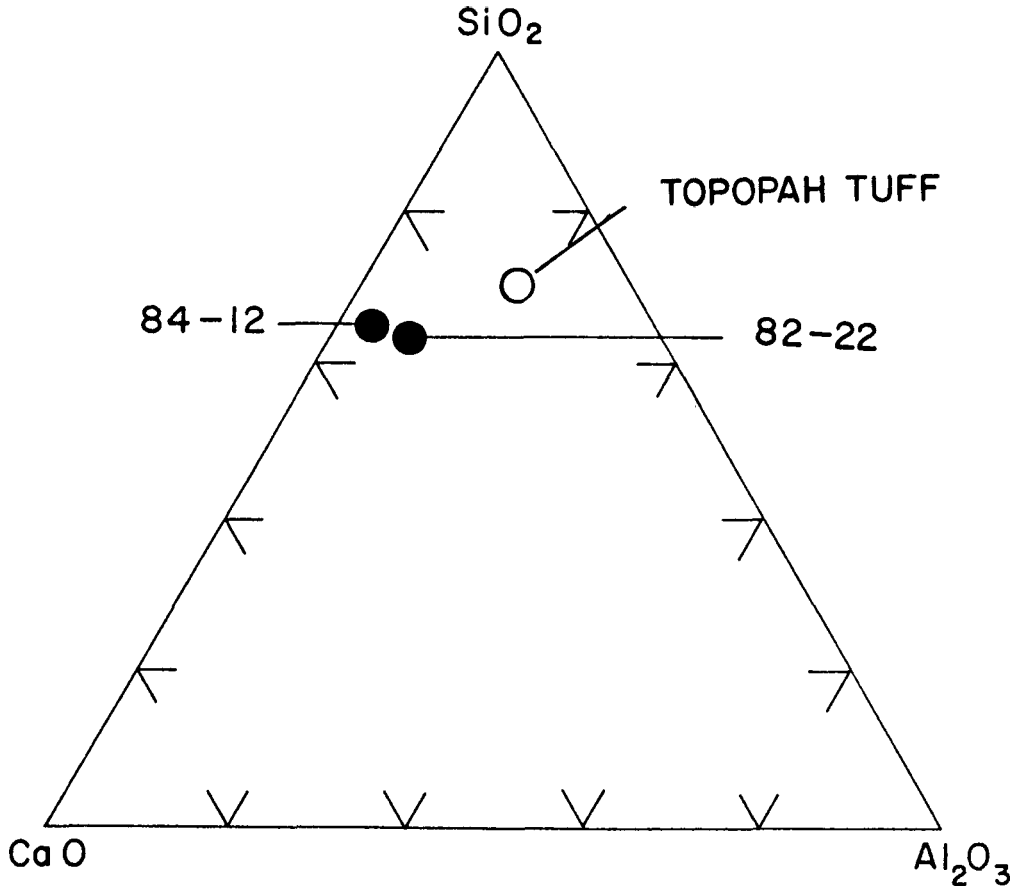

Fig. 3. Bulk chemical composition of tuff, 82-22, and 84-12 mortar normalized to SiO_2 ($+TiO_2+P_2O_5$) - CaO (+alkali and alkaline earth oxides) - Al_2O_3 ($+Fe_2O_3$); neglects SO_3. (See Table I for bulk oxide composition.)

2.4.1 Static Experiments

To evaluate the potential interactions between tuff of the Topopah Spring Member and 82-22, monolithic samples approximately 2-4 mm thick were cut from 50.8-mm-diam cylindrical samples. The cylindrical samples were prepared by casting a prism of tuff (25.4 mm square in cross section) into the center of a cylinder of 82-22 grout. The cut specimens were immersed in the liquid and exposed at temperature and pressure for different time intervals, depending upon the temperature of the experiment. Times ranged from 1 week to 8 months. Experiments were conducted at 90, 150, 200, and 300°C. Fluid

TABLE VIII

SUMMARY OF MATERIALS AND TEST CONDITIONS

	Sample Description	EXPERIMENT TYPE Temperature	Time	Pressure
		AGITATED		
A.	-20+30[a] mesh particles Grouse Canyon tuff mixed 2:1 with 82-22	200°C	to 1000 hrs	3.5 MPa
B.	-20+30 mesh particles Topopah Spring tuff mixed 2:1 with 82-22	150°C	to 800 hrs	sat stm
C.	-20+30 mesh particles Topopah Spring tuff mixed 2:1 with 84-12	200°C	to 600 hrs	sat stm
D.	-20+30 mesh particles Topopah Spring tuff mixed 2:1 with 84-12	150°C	to 300 hrs	sat stm
		STATIC		
E.	5-cm-diam discs of 82-22 cast with Topopah Spring tuff prism	300°C	to 4 weeks	3.5 MPa
	"[b]	200°C	to 8 months	3.5 MPa
	"	150°C	to 3 months	sat stm
	"	90°C	to 3 months	sat stm
		VAPOR PHASE		
F.	5-cm-diam discs of 82-22 cast with Topopah Spring tuff prism	200°C	to 3 months	sat stm
	"	150°C	to 4 months	sat stm
	"	90°C	to 3 months	sat stm

[a]-20+30 mesh particles range from 840 to 590 μm.

[b]Sampled at temperature.

samples were obtained from all of these experiments at the end of the experiment after the reaction vessel was allowed to cool to room temperature. In the 200°C experiment, fluid was sampled at the experimental temperature, as well as at room temperature. Disc samples were removed from all experiments after cooling and the surface alteration was characterized. J-13 groundwater was utilized as the fluid.

2.4.2 Agitated Experiments

Agitated hydrothermal experiments were conducted in a rocking 0.3-ℓ autoclave at 200 and 150°C for "artificial" concretes with both 82-22 and 84-12 grouts. The "artificial" concretes consisted of mechanical mixtures of -20+30 mesh sieve (840- to 590-μm) powders of Topopah Spring tuff (Grouse Canyon tuff in only one case) and the grout in a ratio of 2 parts tuff to 1 part grout. The formulations are summarized in Fig. 2. J-13 groundwater was used as the fluid in all experiments. A water-to-solids ratio of 10:1 was maintained throughout. The techniques are further described in Scheetz and Roy (in preparation).

2.4.3 Simulated Vapor-Phase Experiments

Experiments were designed to approximate the environment of an unsaturated geological zone in the laboratory. Discs of mortar with prisms of tuff cast into the core of the cylinder (similar to those described in Sec. 2.4.1) were suspended in an autoclave above J-13 groundwater and maintained at temperature and saturated steam pressure. Because a thermal gradient exists within these autoclaves, this experiment is somewhat like a mild reflux condenser system in which the fluid is vaporized in the hot end of the system, transported to the cold end of the cell, and condensed. Condensation would occur on the surfaces of the concrete discs and eventually return to the reservoir of J-13 water in the hot end of the vessel. The effect of this design is to provide a situation in which a very low water-to-solids ratio exists on the surface of the disc and is periodically replenished with "fresh" liquid.

3. RESULTS AND DISCUSSION

3.1 Mechanical and Physical Properties of the Grouts

Mechanical and physical property measurements for this mortar formulation have been reported by Roy et al. (in preparation). Compressive strengths of standard 50.8-mm

cubes of 82-22 mortar were determined after the mixture was cured at 38, 60, and 90°C for up to 180 days, according to ASTM C 109. Almost all strengths were found to be above 100 MPa after 7 days, increasing to 130 MPa, a very high strength, at 6 months. Comparable strength for 84-12 after curing at 38°C ranged from 87 to 117 MPa after 28 days of curing. Static Young's modulus values for 82-22 generally increased with time, reaching 9.9 GPa and 8.9 GPa after 180 days of curing at 38 and 60°C, respectively, compared to 8.3 GPa for 84-12 after 28 days at 38°C. Permeability was reported for tuff samples, mortars, and for split-cylindrical samples (half tuff and half mortar). The composite split-cylinder samples generally had permeabilities as low as the tuff samples, in the microdarcy (10^{-18} m^2) range. The mortars generally exhibited no flow, $<10^{-2}$ microdarcy ($<10^{-20}$ m^2).

3.2 The XRD Phase Characterization

Detailed characterization via bulk XRD methods indicated the presence of ettringite, quartz, remnant anhydrous cement phases, and poorly crystallized C-S-H (calcium-silicate-hydrate) in the samples of 82-22 from 7 to 180 days after casting. The relative amounts of the remnant cement phases and the C-S-H, however, changed with time. The anhydrous cement phases decreased markedly, and the C-S-H increased. All samples cured at 38 and 60°C fit this pattern. The samples cured at 90°C contain similar phases, but without ettringite. No corresponding crystalline phases identified as decomposition products of ettringite were detected. It is possible that the sulfate is contained in solid solution in one of the other phases, such as C-S-H at 90°C. The XRD pattern for 84-12 was dominated by peaks caused by quartz sand, with remnant cement phase and poorly crystalline C-S-H peaks composing the remainder of the pattern. The results are summarized in Table IX.

3.3 Results of Elevated-Temperature Studies of 82-22 Mortar with Tuff

For each of the experiments described in the following sections, discs were used that contained a prism of tuff of the Topopah Spring Member cast into the center of a 50.8-mm-diam cylinder and cured for 6 months at 38°C. Each disc was reacted at the described temperature and pressure for a specified time interval and then sampled. The discs were sectioned and approximately half of each disc was dried at 105°C for 24 hours

TABLE IX

BULK XRD CHARACTERIZATION OF 82-22, BEFORE ELEVATED-TEMPERATURE REACTION EXPERIMENTS

	Curing Temperature (°C)			
	82-22			84-12
Time (days)	38	60	90	38
7	e,q,rc,csh[a]	–	q,rc,csh	q,rc,csh
14	–	–	–	q,rc,csh
28	e,q,rc,csh	e,q,rc,csh	q,rc,csh	q,rc,csh
56	e,q,rc,csh	–	q,rc,csh	q,rc,csh
90	e,q,rc,csh	–	q,rc,csh	q,rc,csh
180	e,q,rc,csh	e,q,rc,csh	–	–

[a] e = ettringite, q = quartz, rc = remnant cement phases (C_2S, C_3S, C_4AF), csh = C-S-H. Abbrev: C = CaO, S = SiO_2, H = H_2O, A = Al_2O_3, F = Fe_2O_3.

in preparation for examination in the scanning electron microscope (SEM) or electron microprobe. The remaining half of each disc was retained for bulk XRD studies.

3.3.1 Vapor-Phase Simulations

Four disc samples were prepared for each of three temperatures, 90, 150, and 200°C. Sampling times were scheduled at monthly intervals up to 4 months. At sampling time, the vessel was cooled to room temperature, a fluid sample and a disc were removed, and the vessel was resealed and returned to temperature. Changes in solution chemistry were followed with time.

3.3.1.1 Characterization of Solid Reactants

Microscopic examination of the surfaces of the discs recovered from the 200°C experiment revealed limited surface reaction. Observations on the 1- to 3-month samples suggest that surface alteration occurred about condensed droplets of fluid (Fig. 4) that were distributed randomly over the surface of the disc. However, examination of the

second disc showed that the alteration was associated with the sand-size aggregate in the mortar (Fig. 5). The alteration is composed of euhedral crystals covering the surface of the exposed sand grains. On those sand grains that were not completely covered, as in Fig. 5, etching of the quartz is apparent.

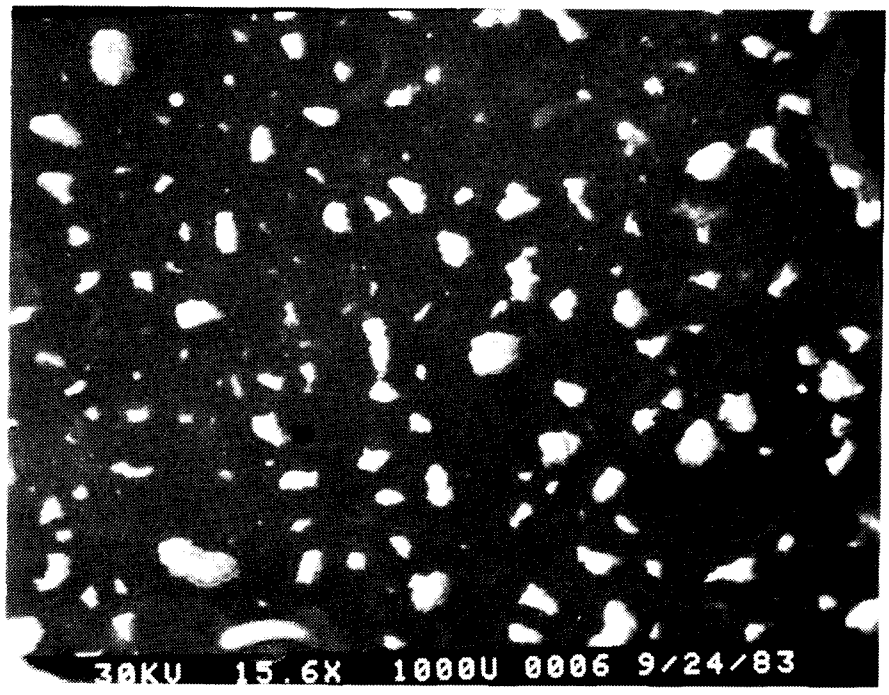

Fig. 4. Distribution of reaction products on the surface of 1-month sample.

Energy-dispersive x-ray (EDX) analysis examination of the crystals developed on these grains revealed a chemistry dominated by calcium and silicon with subordinate amounts of aluminum. The crystal habit was largely fibrous, suggesting tobermorite (Fig. 6a). Occasional patches of well-formed rhombohedral crystals were also observed (Fig. 6b). These were identified as calcite because of their crystal habit and the EDX chemical analyses, which only showed calcium. Carbon and oxygen are not detected by EDX.

Quantification of the bulk chemical composition of these crystals was attempted with an ETEC electron microprobe. However, the results are somewhat uncertain, because

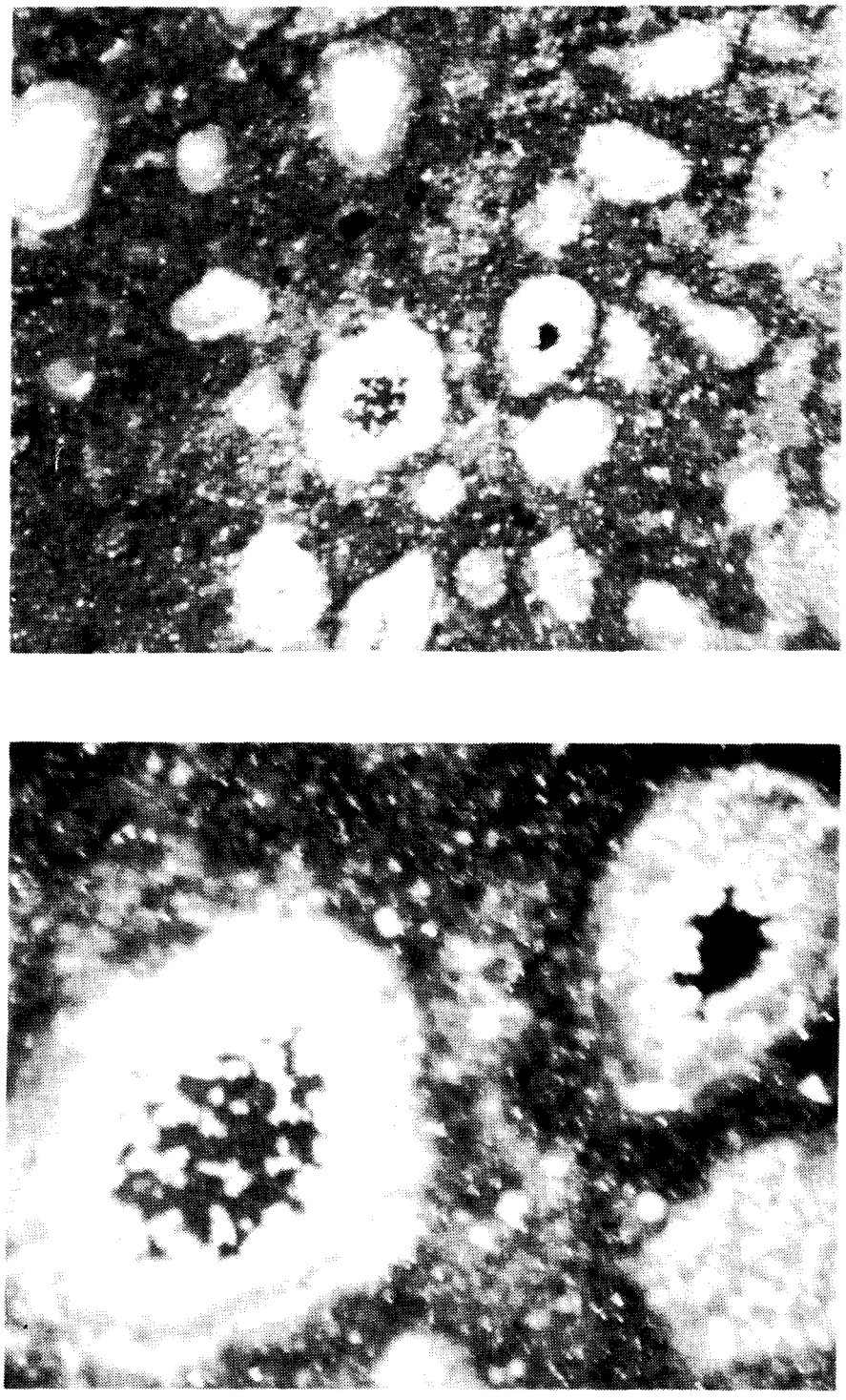

Fig. 5. Surface of 82-22 disc with prism of tuff of the Topopah Spring Member; (b) is an enlargement of the central portion of (a). Alteration occurred associated with the sand-size aggregate on 1-month exposure to 200°C water vapor.

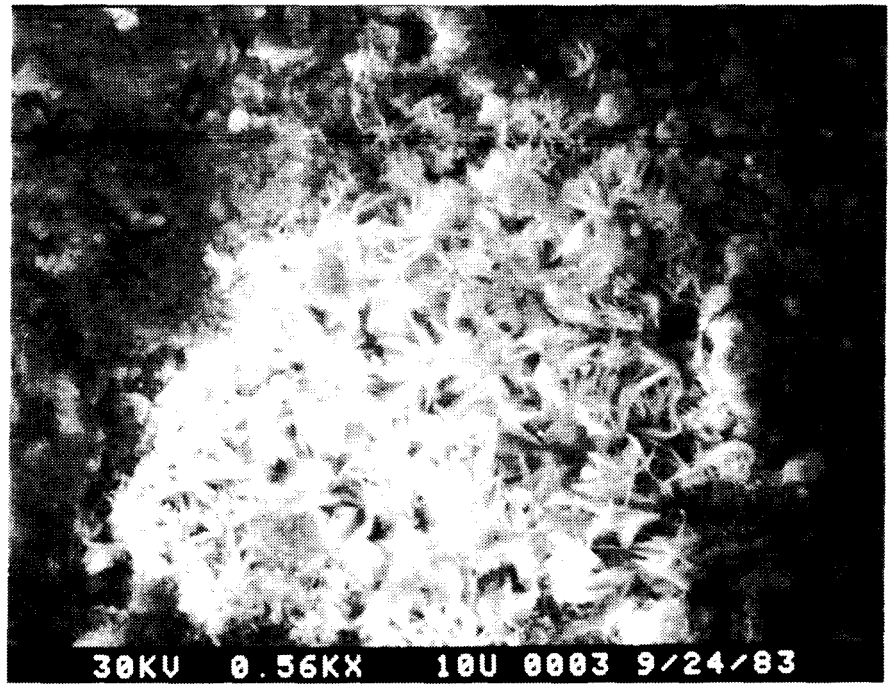

a

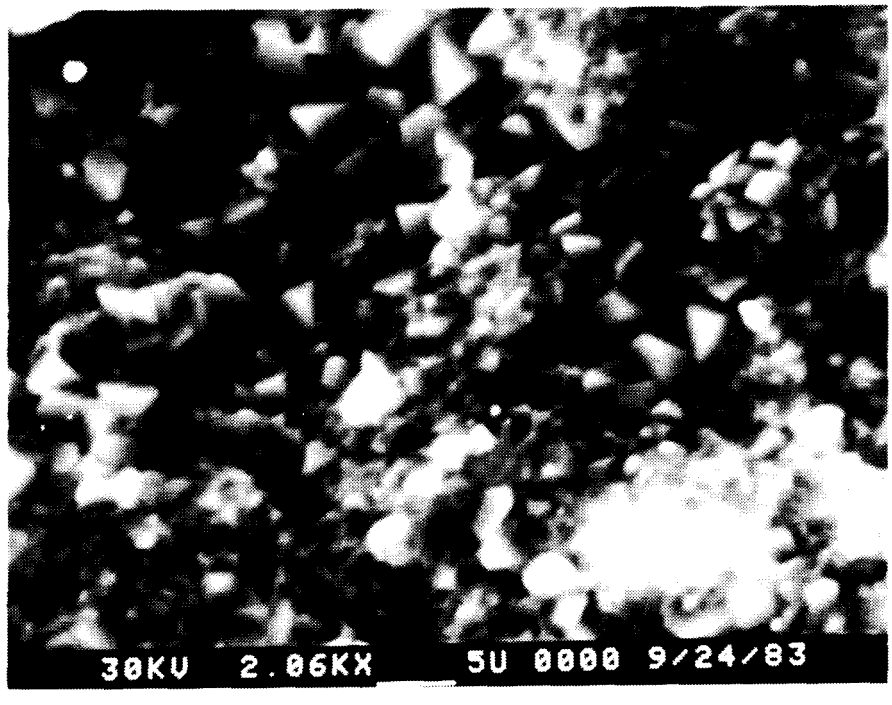

b

Fig. 6. Crystal growth on surface of 82-22 disc with prism of tuff of the Topopah Spring Member. Sample exposed 1 month to 200°C water vapor.

of the rough nature of the surface. Use of anything but a well-polished, flat specimen can produce misleading results caused by uncontrolled losses of x-ray signal from the surface and variable density of the bulk specimen being analyzed. Table X summarizes the compositions of the crystals, which have atomic ratios of calcium to silicon varying from 1.16 to 1.45.

TABLE X

MICROPROBE ANALYSIS OF 200°C DISCS OF MORTAR 82-22 AND TOPOPAH SPRING TUFF EXPOSED TO CONDENSING VAPOR OVER J-13 GROUNDWATER

	Weight % (2σ)							
Element	#1		#2		#3		#4	
Mg	0.32	(0.11)	0.14	(0.10)	0.17	(0.10)	0.10	(0.10)
Al	0.67	(0.09)	0.72	(0.09)	0.50	(0.09)	0.60	(0.10)
Si	14.73	(0.19)	17.31	(0.22)	16.73	(0.21)	15.73	(0.20)
S	0.34	(0.08)	0.29	(0.77)	0.24	(0.06)	0.20	(0.06)
K	0.55	(0.08)	0.61	(0.08)	0.70	(0.08)	0.64	(0.08)
Ca	30.78	(0.44)	28.68	(0.41)	31.47	(0.45)	32.30	(0.47)
O[a]	30.49		32.45		32.69		31.85	

[a]Determined by stoichiometry.

Bulk XRD performed on the undried half of the original treated discs by placing the disc into the sample position of a standard powder diffractometer detected the alteration products tobermorite, calcite, quartz, and an unidentified phase.

A very well developed transition zone approximately 2 to 2.5 μm wide exists between the tuff and the host mortar. Examination of this zone by SEM using EDX and the electron back scattering (EBS) detector revealed that the transition zone is dominantly calcium and silicon in a ratio of about 3:1, which is consistent with a calcium-silicate-hydrate. The crystals in Fig. 7 grew into a void space in the tuff. The phase may be $Ca_6Si_2O_{10} \cdot 3H_2O$. The phase hexacalcium disilicate trihydrate possesses a hexagonal morphology with crystal

development along the c-axis (Taylor, 1964) and has been observed to form between 180° and 350°C under saturated steam pressure, as a reaction product of Ca_3SiO_5. This appears to be a transition phase and is not observed in longer experiments, because of the bulk composition of the system.

Fig. 7. Crystal growth at interface between 82-22 and tuff of the Topopah Spring Member.

Chemical profiling across the interface was conducted at two different magnifications. The first at 50X produced a total traverse of 1800 μm. The second at 500X produced a traverse of 180 μm. These two traverses are presented in Figs. 8 and 9, respectively. The accompanying SEM/EBS image in Fig. 8 contains the mortar to the left of the image. The large subrounded patches are quartz sand aggregate. The calcium-to-silicon ratios in the mortar are approximately 1:1. Points 2 and 3 of the profile intercept a sand grain accounting for the very large number of silicon x-ray counts. The section through the interfacial region did not traverse a segment that possessed a very strongly developed

interfacial zone. Only a very faint enrichment in calcium can be identified in the EBS image in Fig. 8 in the contact zone at point 13. Point to point separation at this scale is 56.25 μm.

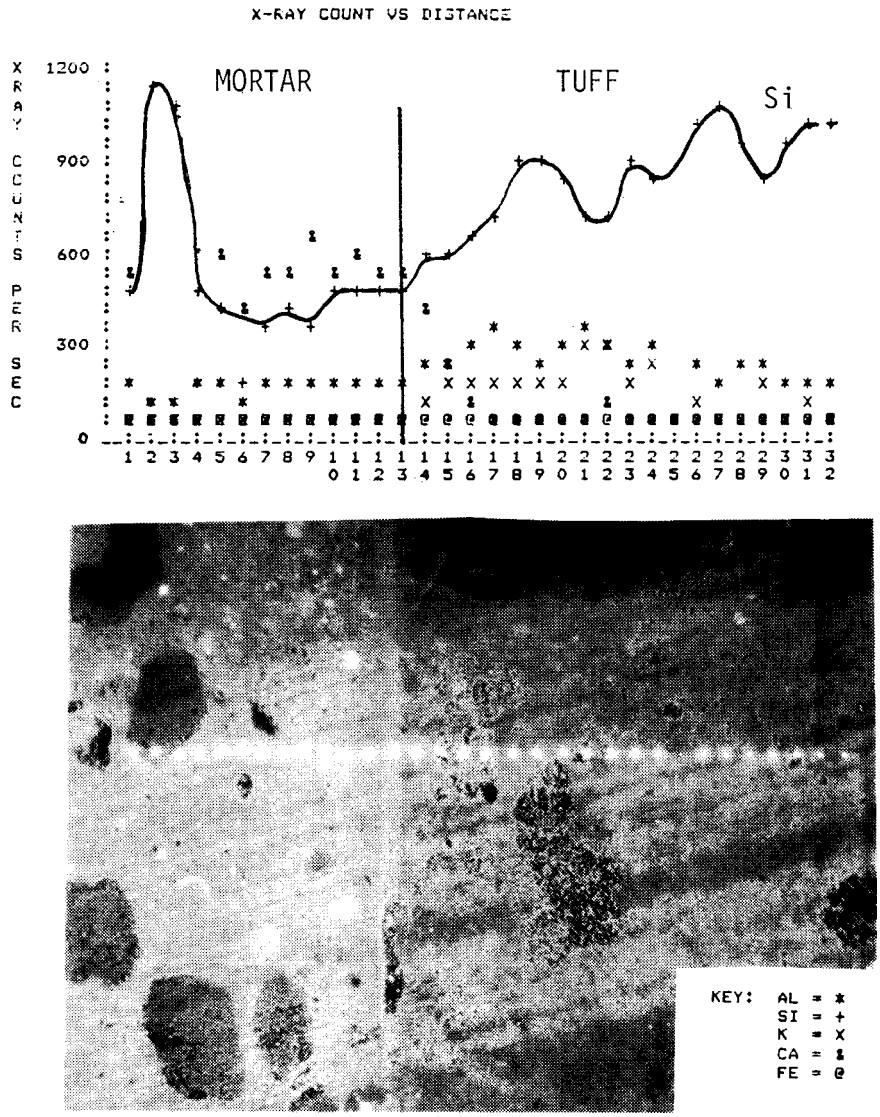

Fig. 8. Traverse, SEM/EBS of 82-22/tuff interface, 50X; total traverse, 1800 μm.

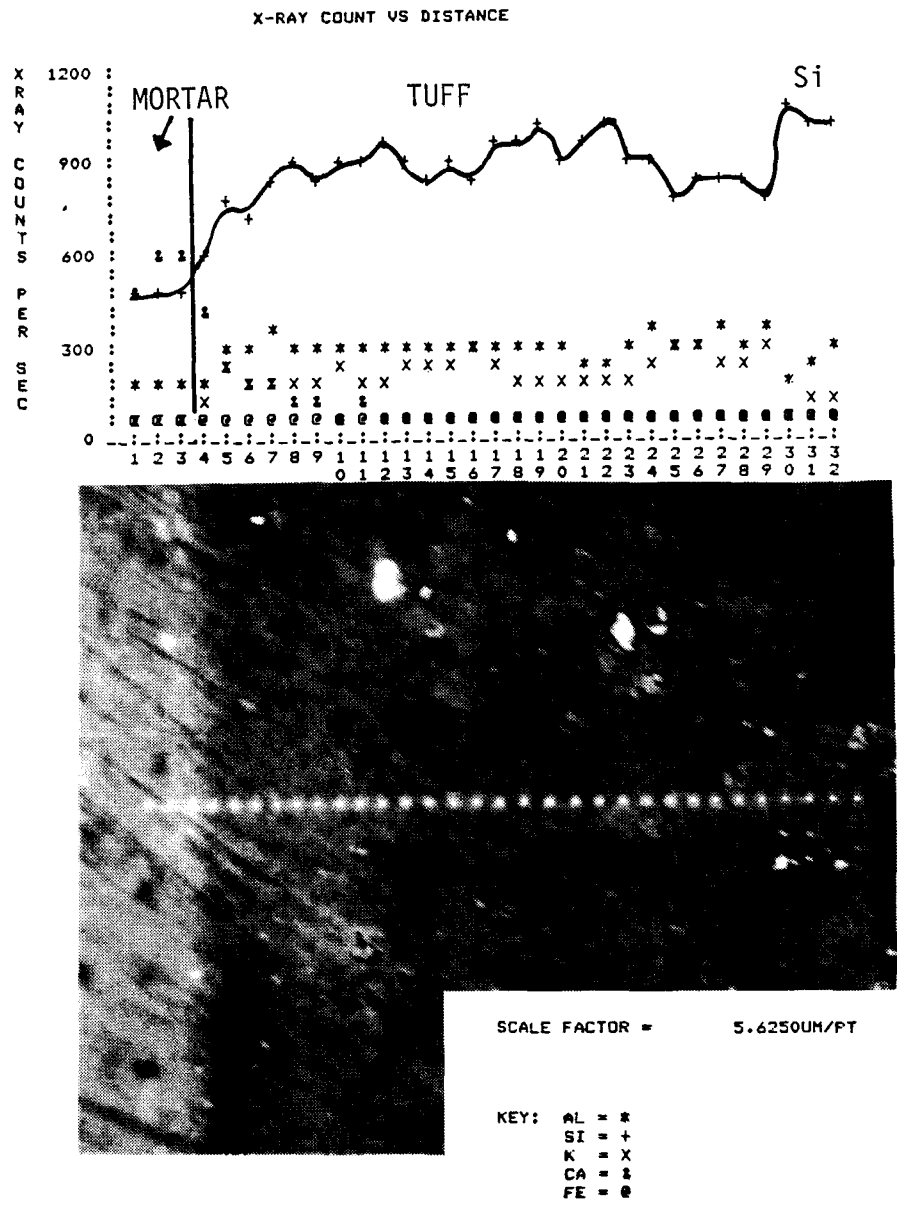

Fig. 9. Traverse, SEM/EBS of interface, 500X; total traverse, 180 μm.

Entrance into the prism of Topopah Spring tuff is marked by a gradual increase in the silicon and potassium x-ray counts and a complementary decrease in the calcium x-ray counts. There appears to be a zone between 169 and 225 μm wide between the mortar and the unaltered tuff that is depleted in silicon and potassium. The size of the symbols in Figs. 8 and 9 corresponds roughly to the $N^{1/2}$ counting error.

Figure 9 shows a traverse of a different region of the interface at a point to point separation of 5.62 μm. In this figure, as in the previous one, no well-developed interfacial zone is observed; however, if the silicon and potassium signals are followed, a transition zone approximately 25 to 30 μm wide can be identified. The difference between these two observations may reflect the more detailed traverse of the second figure (the entire traverse in Fig. 9 is equal to the distance traversed in the interfacial zone in Fig. 8).

Characterization of the surface of the disc exposed to 150°C vapor, like those exposed at 200°C, reveals extensive development of well-crystallized tobermorite (Fig. 10) and the presence of micrometer-size euhedral crystals of calcite (Fig. 11) (identified by morphology and EDX chemistry of calcium only) within the platy tobermorite. The XRD of the surfaces of the disc samples confirms that these are the dominant phases.

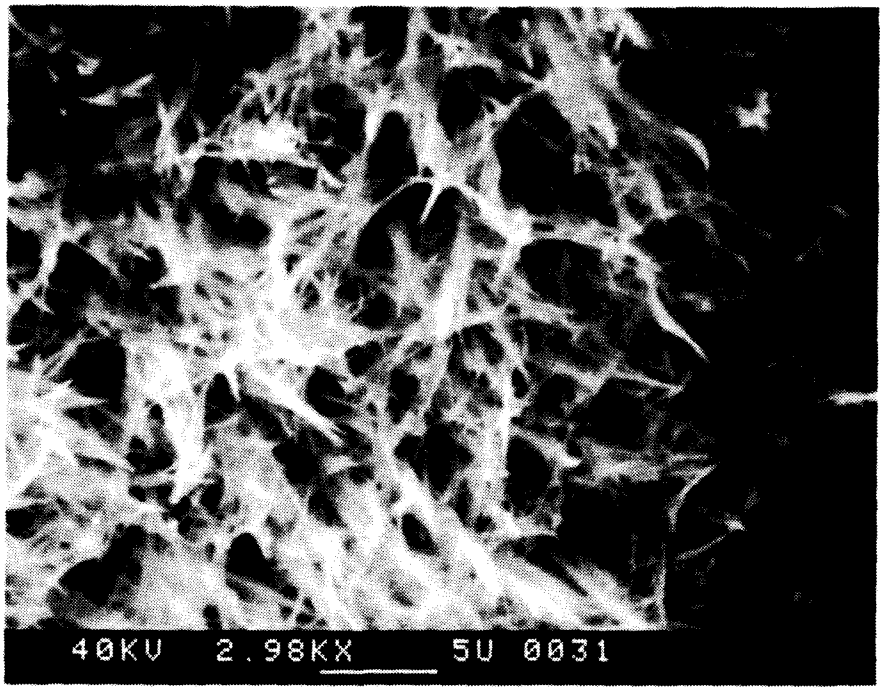

Fig. 10. Tobermorite fibrous crystal growth on 150°C disc.

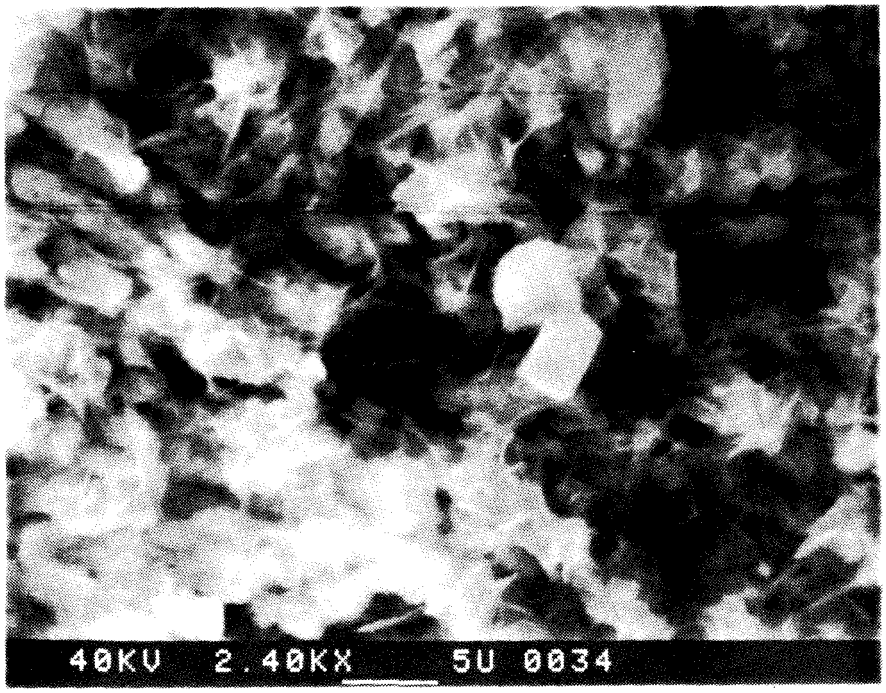

Fig. 11. Euhedral calcite crystals among platy tobermorite crystals on 150°C disc.

The third set of samples was exposed to 90°C water vapor for up to 3 months. The surface alteration on this set of samples was distinctly different from those just described. Instead of tobermorite, the crust that developed was dominantly calcite (Fig. 12). The XRD confirmed the presence of calcite along with tobermorite, quartz, and feldspar from the bulk specimen. This treatment probably exposed the samples to greater exchange with atmospheric CO_2.

3.3.1.2 Characterization of Liquid Phase

The solutions that were removed from these sets of experiments were analyzed for 15 cations and anions. These analyses indicate that the solution chemistry is dominated by calcium, sulfate, silicon, sodium, and potassium. These data are presented in Appendix A. No consistent patterns exist in the data.

3.3.2 Static Saturated Experiments

Sample-preparation procedures followed in this set of experiments were similar to those in the vapor-phase series. Discs of 82-22 grout with prisms of tuff of the Topopah Spring Member cast in the centers were reacted at 90, 150, 200, and 300°C and saturated

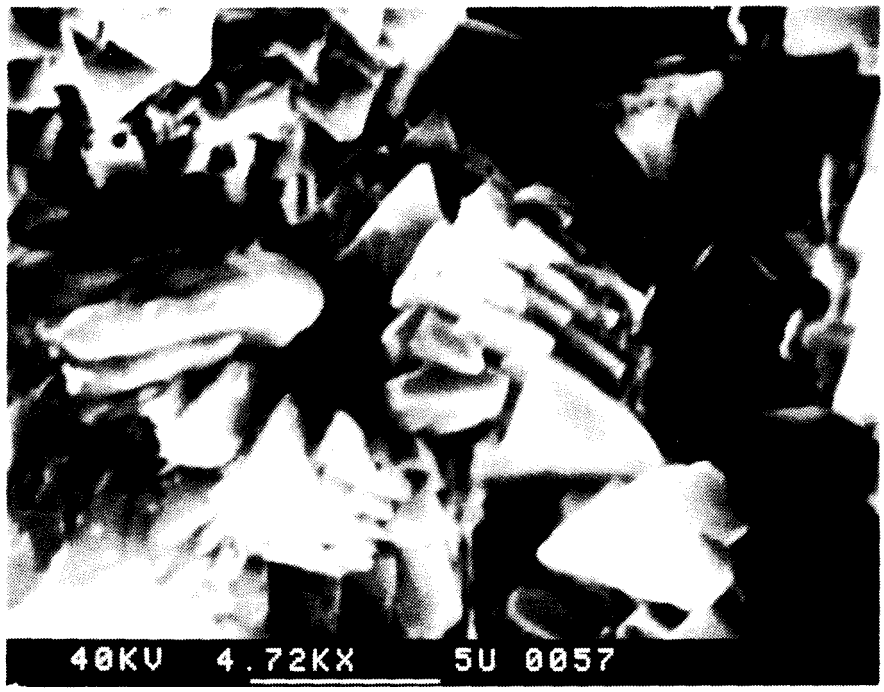

Fig. 12. Euhedral calcite crystals on surface of 90°C disc.

steam pressure or 3.5 MPa (see Table VIII details) for time intervals up to 8 months. At sampling time, the vessel was cooled to room temperature, and a disc and a solution sample were recovered. The remaining samples were returned to the test conditions.

3.3.2.1 Characterization of the Solid Samples

The first sample in this set was run at 200°C for 6 days followed by 300°C for 1 full day. Subsequent samples were maintained at the upper temperature and were sampled at 2^n weeks, starting at 1 week.

At one week, needle-like crystals, identified by XRD as tobermorite, had formed. The second week, a more platy structure was observed. These observations are illustrated in Fig. 13a and b. Table XI summarizes the results of microprobe analyses of the crystals. The molar ratio of calcium:silicon was 0.80 at 1 week, and 0.63 at 2 weeks, consistent with tobermorite and truscottite, respectively. At 4 weeks, hexagonal or pseudo-hexagonal platy truscottite was observed (Fig. 14). High-symmetry dodecahedral/trapezohedral crystals that may be hydrogarnet were also observed. The hydrogarnet may have formed as a

decomposition product of ettringite or from calcium aluminate liberated by the reaction of tobermorite to truscottite (Fig. 14 a,b,c).

The contact zone between the tuff and the grout appears to be very tight with no observable gaps (Fig. 15). A sharp chemical boundary was observed by EDX at the interface.

After the initial week of reaction and the excursion to 300°C, a crust was observed that was interpreted as a quench product because of its distribution in the Parr vessel. The phases in this material were identified by XRD as tobermorite, quartz, calcite, portlandite, and an unidentified phase.

The surface of the disc recovered from the 200°C experiment after 1 month was so overgrown with alteration products that they completely covered the original surface. The alteration consisted of fine euhedral fibrous and platy crystals that contain primarily calcium and silicon with subordinate amounts of aluminum ± potassium, iron, and sulfur. Figure 16 is a secondary electron image (SEI) of the crystalline overgrowth that covers the surface of the disc. Tobermorite was identified by bulk XRD as the principal crystalline phase with lesser quartz and calcite and minor truscottite. Electron microprobe data (Table XII) suggest that a small amount of aluminum [up to 0.08 Al/(Si+Al)], a smaller amount of potassium, and possibly a smaller amount of sulfate are substituted into the tobermorite structure. With prolonged exposure to these experimental conditions, tobermorite undergoes alteration by reaction with silica to truscottite.

An interfacial zone rich in calcium and silicon as previously described was noted on these samples.

3.3.2.2 Characterization of Liquid Samples

The analyses of the solutions recovered from these experiments are presented in Appendix B. The pH values recorded at ambient laboratory temperature exhibit a wide, but not systematic, variation with experimental temperature, ranging from about 7.5 for the 300°C experiment to 11.6 for the 150°C experiment. Within any single data set, however, the pH values do not vary more than one pH unit. The pH is lower at higher temperature for a given material. As was seen in the vapor-phase experiments, the solution chemistry is dominated by the presence of calcium, sulfate, silicon, sodium, and potassium.

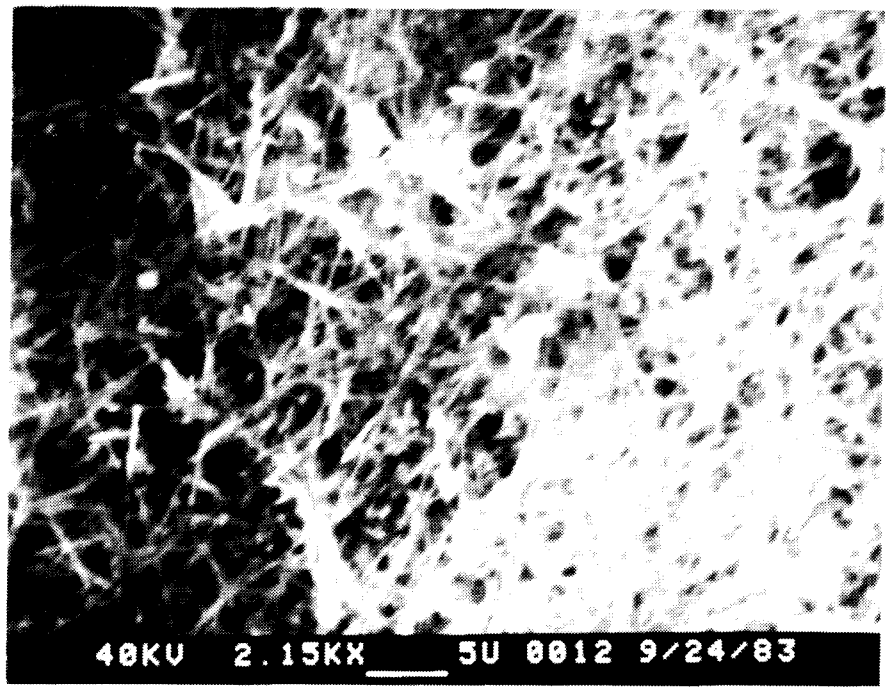

a

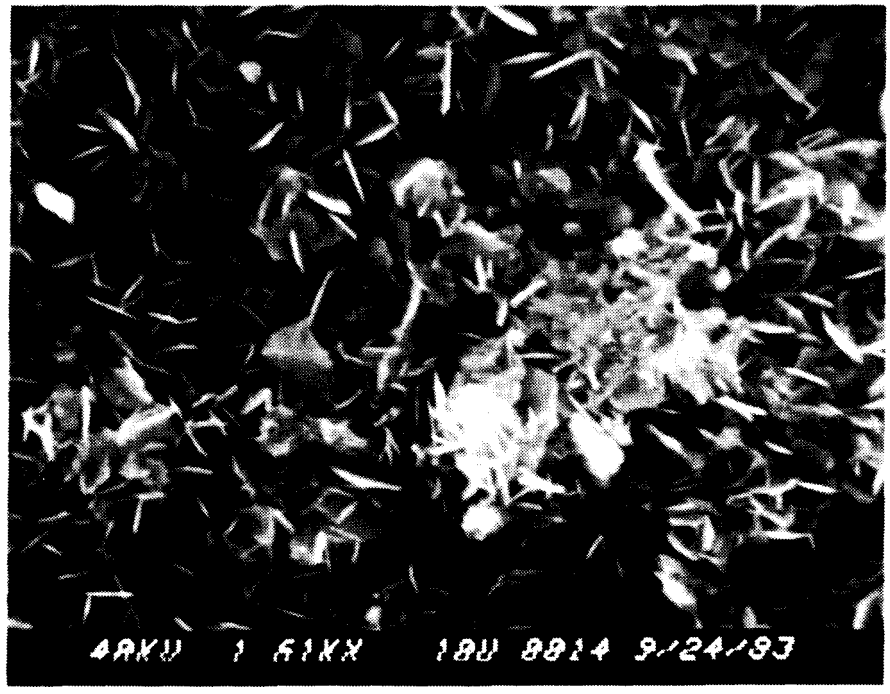

b

Fig. 13. Crystalline development of tobermorite at (a) 1 week and (b) 2 weeks at 300°C.

TABLE XI

MICROPROBE ANALYSIS OF 300°C DISCS OF THE MORTAR 82-22 AND TOPOPAH SPRING TUFF

Element	Weight % (2σ)					
	#1		#2		#3	
	1 Week					
Al	2.72	(0.12)	2.59	(0.13)	3.88	(0.15)
Si	22.92	(0.26)	23.40	(0.26)	22.60	(0.26)
S	0.03	(0.04)	–	–	–	–
K	1.09	(0.09)	0.99	(0.09)	1.11	(0.09)
Ca	26.43	(0.41)	27.01	(0.42)	24.43	(0.38)
Fe	0.18	(0.13)	–	–	–	–
O[a]	39.41		39.96		39.28	
	2 Weeks					
Na	0.13	(0.23)	0.13	(0.10)	–	–
Mg	0.64	(0.12)	0.74	(0.12)	0.18	(0.10)
Al	2.21	(0.13)	2.45	(0.13)	2.36	(0.13)
Si	24.96	(0.28)	26.03	(0.29)	25.07	(0.28)
S	0.92	(0.17)	0.98	(0.18)	0.11	(0.05)
K	2.81	(0.12)	2.47	(0.11)	2.67	(0.11)
Ca	22.53	(0.35)	23.19	(0.36)	22.45	(0.35)
Fe	–	–	–	–	–	–
O[a]	42.38		43.92		40.62	

[a]Determined by stoichiometry.

The data do not exhibit any trends with temperature and many exhibit wide variations in concentration with time.

3.3.3 Rocking-Autoclave Granular-Mixture Experiments

Two sets of experiments were completed in a rocking-autoclave apparatus. The solids used in these experiments consisted of a mechanical mixture of -20+30 sieve (840-

Fig. 14. Surface alteration of 82-22 grout after 4 weeks at 300°C. (a) Platy truscottite, (b) morphological relation between hydrogarnet (?) and truscottite, and (c) possibly hydrogarnet.

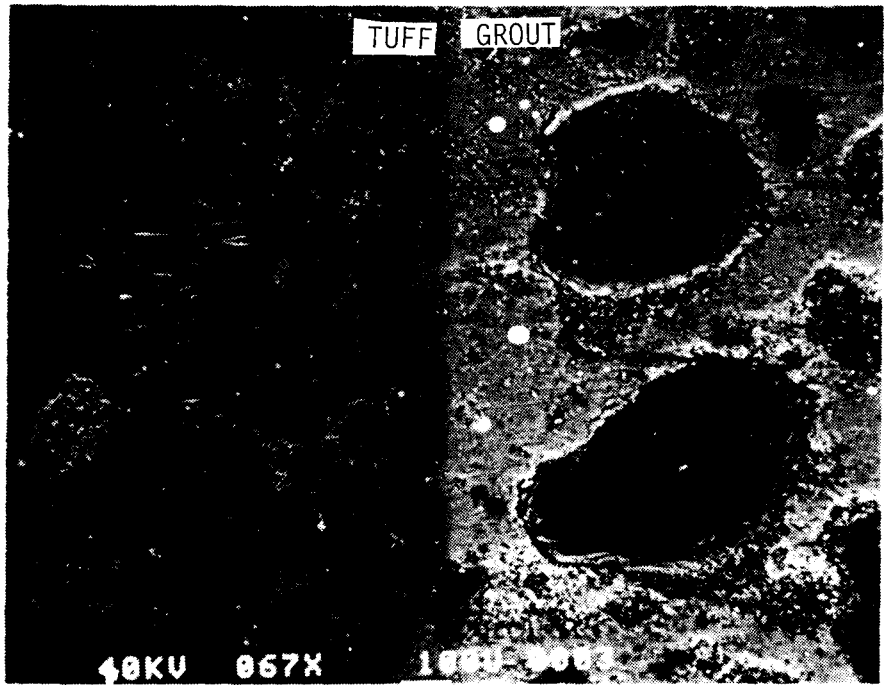

Fig. 15. Interface contact between grout on the right and tuff on the left.

to 590-μm) tuff of the Topopah Spring Member and mature 82-22 or 84-12 mortar. The experiments were conducted at 150 and 200°C on a sampling schedule of t = 2^n hours where n = 0 to 10.

3.3.3.1 Formulation 82-22 + Tuff

Figure 17 presents the chemical analyses of the solutions from the 82-22/tuff experiments (Table VIII, A and B) at 150 and 200°C. All of the data contain the solution analyses for the last sample recovered both at temperature and after the vessel was allowed to cool to room temperature.

The pH of the 150°C experiment (measured at room temperature) was approximately 9.5 for the first 200 hours of the experiment, after which it dropped to about 9.0 by 800 hours and exhibited a large increase to 9.9 after the vessel had cooled to room temperature. The pH of the 200°C experiment was about 8.5 for almost the first 500 hours before it dropped to 6.5. There was only a slight increase in the pH accompanying the thermal quench of the 200°C experiment.

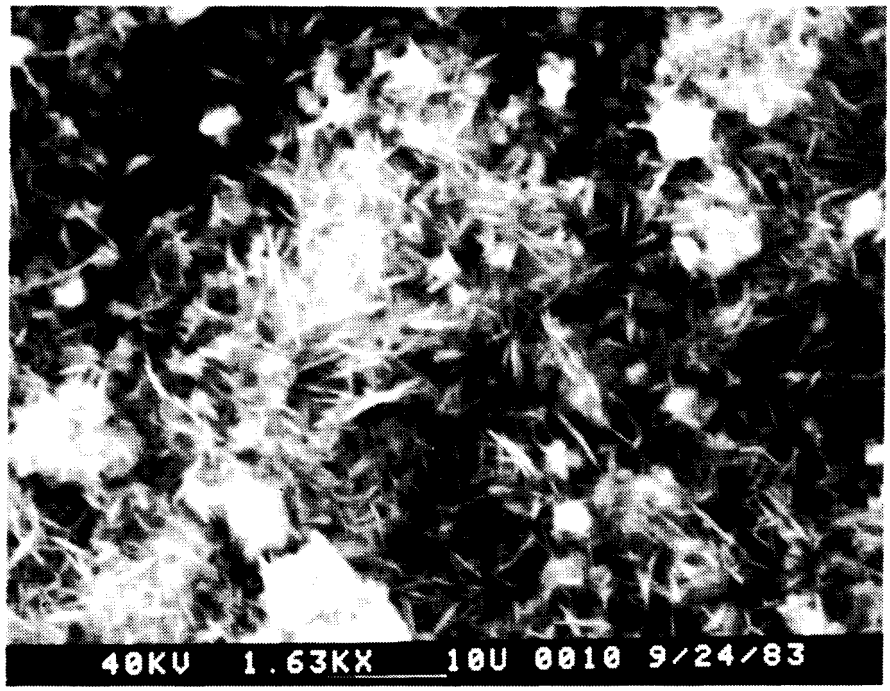

Fig. 16. Development of fibrous tobermorite on the surface of 82-22 tuff sample at 200°C after 1 month of hydrothermal treatment.

With the exception of silicon, the ionic species in the 150°C experiments are present at higher concentration than in the 200°C experiment. The concentration of calcium and sulfate is higher in the fluid sampled at room temperature than in the fluid sampled at the temperature of the experiment, suggesting a retrograde solubility behavior. In both data sets, the calcium concentration (expressed as millimoles of the cation) is always less than that of the sulfate. Silica exhibits an initial increase in concentration followed by a decrease to a relatively constant level and a definite drop upon cooling to room temperature. Finally, sodium exhibits a steady increase in concentration in the fluid and appears to asymptotically approach a fixed value.

3.3.3.2 Formulation 84-12 and Tuff

The results of the fluid-phase analyses of 84-12/tuff mixtures (Table VIII, C,D) are also presented in Fig. 17. The pH for the 84-12 formulation at 200°C averaged 9.7 during the initial 100 hours, after which it dropped to 8.5 at 200 hours. The pH of the 150°C

TABLE XII

ELECTRON MICROPROBE ANALYSIS FOR DISC SURFACE AGITATED AT 200°C FOR 1 MONTH OF HYDROTHERMAL TREATMENT

	Weight % (2σ)							
Element	#1		#2		#3		#4	
Mg	0.06	(0.07)	0.20	(0.10)	0.12	(0.10)	–	–
Al	1.83	(0.11)	1.65	(0.11)	2.13	(0.13)	2.14	(0.12)
Si	22.40	(0.25)	20.54	(0.23)	24.04	(0.27)	25.02	(0.28)
S	0.12	(0.05)	0.14	(0.05)	0.08	(0.04)	0.08	(0.05)
K	0.83	(0.09)	0.76	(0.09)	0.79	(0.09)	0.74	(0.09)
Ca	24.76	(0.39)	21.94	(0.34)	24.34	(9.38)	25.61	(0.40)
O[a]	50.00		54.01		48.50		46.41	

[a]Determined by stoichiometry.

experiment was 9.4 at 2 hours and was maintained at this value for the duration of the experiment.

As for the 82-22 formulation, the calcium and sulfate concentrations mimic each other, with the sulfate concentration approaching twice that of the calcium. The liquid recovered at the termination of the experiment exhibits a sharp increase in the concentration of both calcium and sulfate. There is a steady, slight decrease in silica concentration in solution with time, but the quenched sample taken at room temperature exhibits an unusual increase in concentration. The sodium concentration decreases steadily to about 200 hours (at 200°C) followed by a slight increase in concentration to the termination of the experiment. In the 150°C experiment, the sodium concentration increases with time.

3.3.3.3 Comparison of the 82-22 and 84-12 Formulations

The data represented in Fig. 17 suggest that at both 150° and 200°C a steady-state condition was reached within the first 50 to 100 hours of the experiment. Calcium and sulfate approach similar concentration for both the concrete formulations. The initial

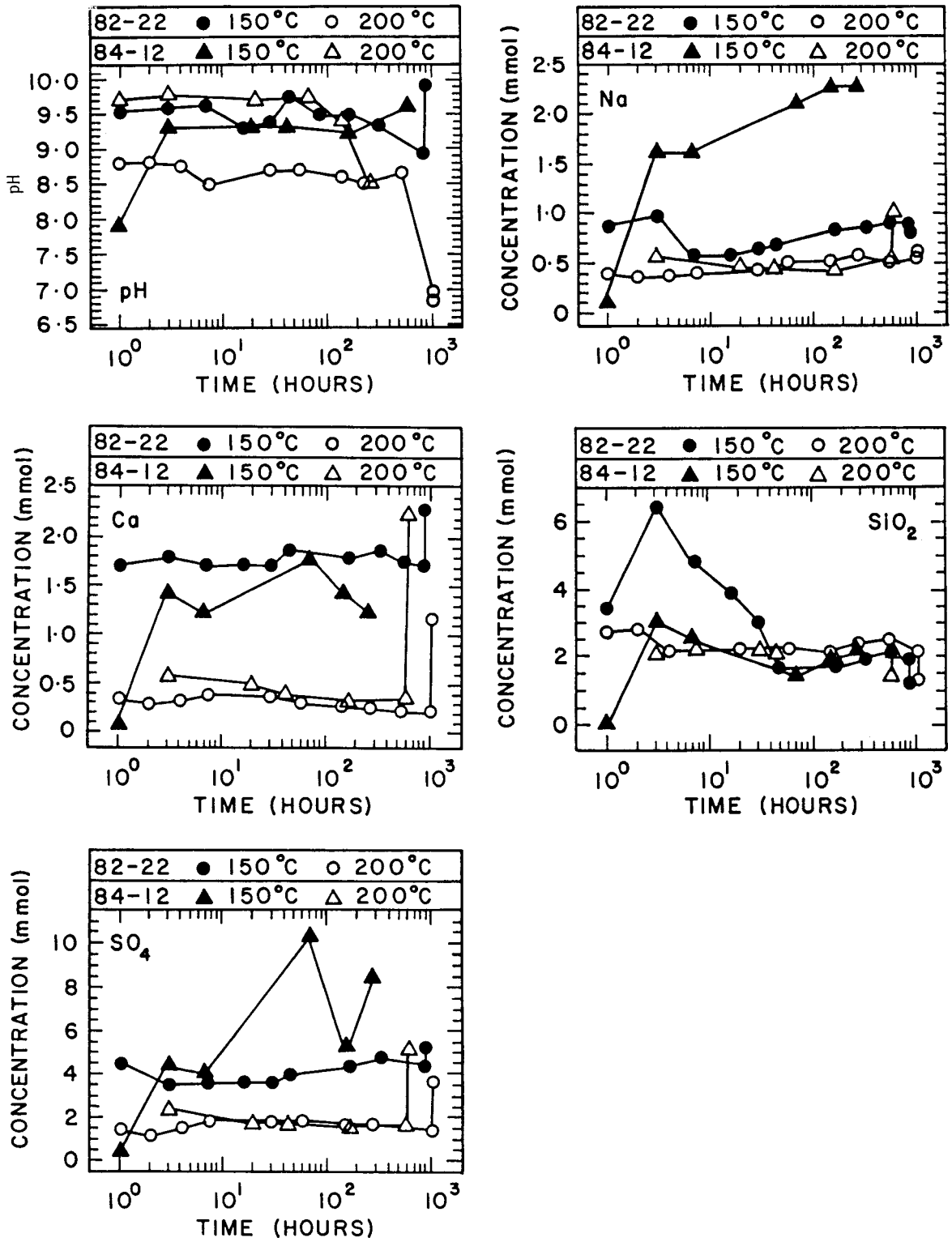

Fig. 17. Concentration vs time plots for each of the dominant ions in the solutions in contact with the "artificial" concrete.

concrete formulation was developed about an expansive matrix, and the latter 84-12 formulation about a nonexpansive formulation. The sulfate concentration in the fluid approaches a similar concentration despite the differing amount of sulfate in the solids. This suggests that equilibrium is being closely approached. The sulfate also exhibits a retrograde solubility behavior, being more concentrated at the lower temperature than at the higher. The relative concentrations observed between calcium and sulfate significantly deviate from 1:1 with the concentration of sulfate averaging about 4 to 6 times that of calcium.

Behavior similar to that described for calcium and sulfate was recorded for sodium. Silica on the other hand exhibits a similar concentration for all of the runs. The 200°C concentration is not much higher than that at 150°C. The values for pH all appear to cluster near 9.50 ± 0.2, with the exception of the 200°C 82-22 experiment, which remained at a value of about 8.7.

Finally, the last data points presented in Fig. 17 exhibit either a sharp increase as in the case of calcium, sulfate, pH, and sodium or a decrease as in silicon. This change represents the response of the solution chemistry to cooling to room temperature.

3.3.3.4 Solids Characterization

The SEM/EDX examination of both the 150°C 82-22 and 84-12 reaction products revealed fibrous crystals with morphologies similar to those previously identified as tobermorite. Bulk XRD of the 150°C 82-22 reaction products confirmed that tobermorite was the dominant phase. Reaction products in the 200°C 82-22 and 84-12 experiments possessed a platy morphology typical of truscottite. Also present were calcite plus quartz and feldspar. No microprobe data were collected for these crystals. Figure 18a and b represent the fibrous crystals with patches of the platelets in 18a clearly visible; Fig. 19a and b detail the platelet crystal morphology.

4. SUMMARY

In the current experiments, poorly crystalline C-S-H has altered primarily to tobermorite, $Ca_5Si_6O_{16}(OH)_2 \cdot 4H_2O$. Accompanying changes occur in some of the minor constituent phases. Alteration of tobermorite to truscottite has been observed in some of the higher temperature experiments.

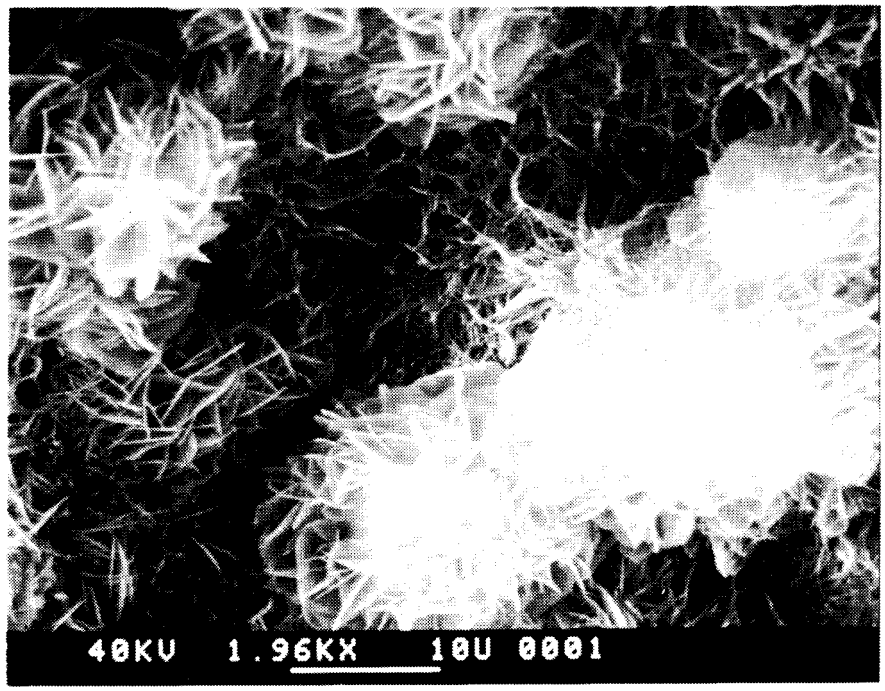

a

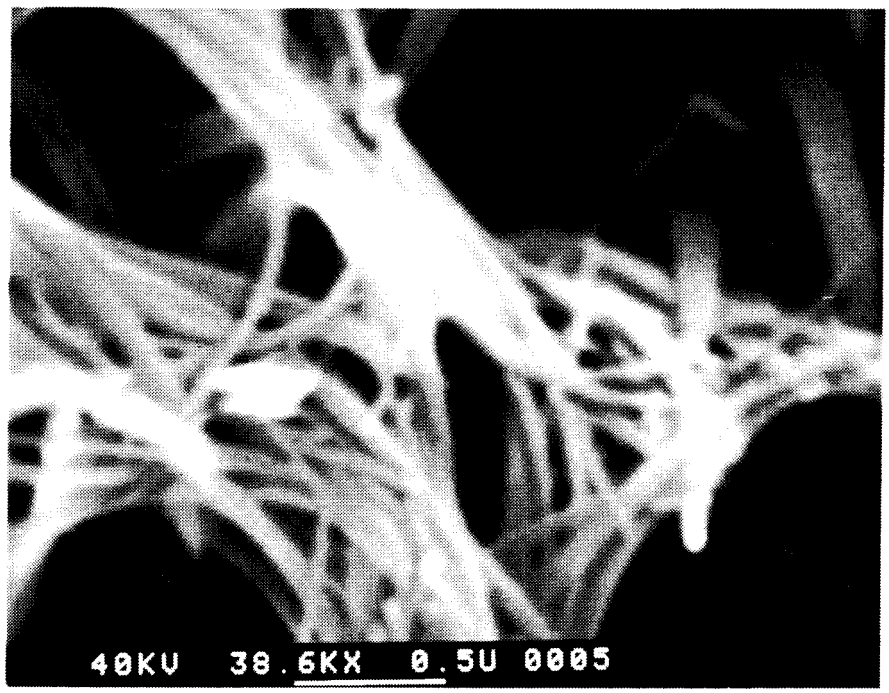

b

Fig. 18. The SEM (SEI) images of reaction products from 200°C 82-22 rocking-autoclave experiments showing the fibrous/platy habit of tobermorite.

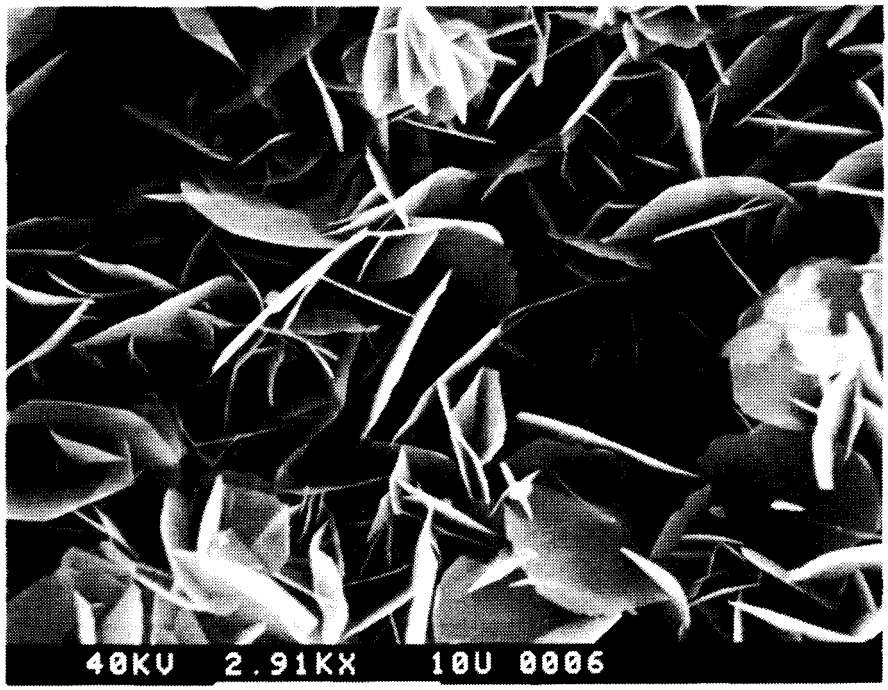

a

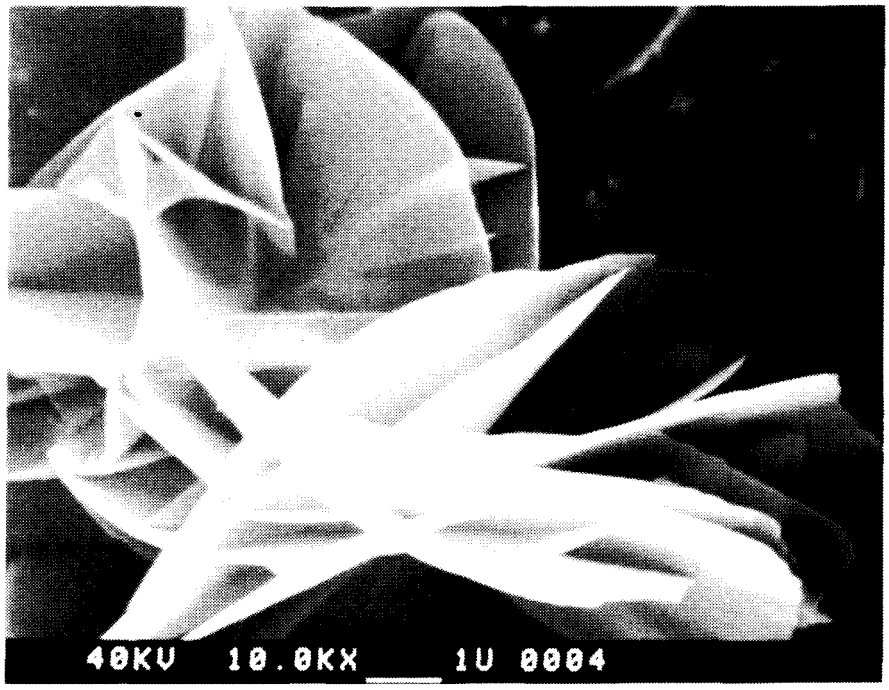

b

Fig. 19. The SEM (SEI) images of reaction products from 200°C 82-22 rocking-autoclave experiments showing the platelet habit of truscottite.

The dominant product of the elevated temperature alteration of the grout formulations 82-22 and 84-12 with tuff is tobermorite, a naturally occurring mineral phase that is reputed to be structurally related to C-S-H. In autoclaved concrete building products, tobermorite is the chief binding phase and is known to produce stable, strong materials. The grouts were designed with a bulk chemical composition that could form dominantly tobermorite or a mixture of tobermorite plus gyrolite or truscottite, depending upon how much of the coarser siliceous sand fraction reacted. The low-temperature C-S-H and calcium hydroxide formed initially during the portland cement hydration and aging of samples have reacted with siliceous components at elevated temperatures to form dominantly tobermorite, with minor gyrolite or truscottite.

The experiments that are reported all exhibit the presence of tobermorite, even in the 300°C experiments. The presence of tobermorite at high temperature may be due to incorporation of aluminum in its lattice. Early crystal chemical studies of aluminum substitution into the tobermorite structure by Kalousek (1957), Roy and Johnson (1965), Diamond et al. (1966), and more recent studies by Komarneni, Roy, and Roy (1982) and Komarneni and Roy (1983a,b) suggest that the incorporation of aluminum in the structure will increase the thermal stability. The latter authors also show the advantages of coupled alkali plus aluminum substitution in tobermorite, which generates a material having ion exchange properties giving excellent radionuclide sorption.

Komarneni and Roy (1983a,b) synthesized aluminum-substituted tobermorites at 180°C from bulk compositions in which the atomic ratio of Al/(Al+Si) was equal to 0.1. No aluminum-rich secondary phase was found in the reaction product, suggesting that all the Al was incorporated in the tobermorite structure. This finding agrees well with the electron microprobe analyses of surfaces of 82-22 (tobermorite), which show Al/(Al+Si)=0.09 at 200°C and Al/(Al+Si)=0.10 at 300°C, except for a single 300°C sample having a higher ratio of Al/(Al+Si)=0.17.

Mixture 84-12 contains a higher proportion of alumina, which could form more aluminum-substituted tobermorite from the cementitious matrix components. In both cases (82-22 and 84-12), there is abundant SiO_2 remaining after formation of tobermorite, so that slow reaction can take place to form the silica-rich phases, gyrolite or truscottite.

The composite samples of 82-22 and 84-12 with tuff of the Topopah Spring Member appear intact. No mechanical discontinuities (cracks) can be seen between the tuff and the mortar after elevated temperature/pressure exposure.

These results suggest that at these elevated temperatures the cementitious matrix in both mixtures 82-22 and 84-12 reacts within itself to produce tobermorite. That is, the calcium-rich portland cement and siliceous and aluminous components combine to produce crystalline aluminum-substituted tobermorite. At 200°C and above, tobermorite was observed to be partially reacted with the excess silica to form truscottite.

Characterization of the solid reaction products in all of these experiments has revealed the general appearance of a common suite of crystalline phases, regardless of the initial bulk chemistry of the constituents of the grout. The presence of very reactive silica admixtures has resulted in the formation of additional C-S-H gel, which under the thermal conditions of these tests has converted into crystalline tobermorite. This cementitious phase is formed at the expense of the less desirable portlandite that is formed from formulations less silica rich than tobermorite. The availability of carbon dioxide results in the ubiquitous formation of calcite, even in the presence of excess silica.

The instability of ettringite, the phase responsible for the expansive behavior of the 82-22 grout formulation, at elevated temperatures above 90-120°C is responsible for the lack of observation of this phase in any of the elevated-temperature experiments. Curiously, no decomposition products of ettringite were observed, with the possible exception of the high-symmetry cubic crystal in Fig. 14c, which may be hydrogarnet. The presence of tobermorite in experiments at temperatures up to 300°C may be due to incorporation of aluminum into the structure and a slow rate of reaction with quartz. At longer times, the reaction

$$\text{tobermorite} + \text{quartz} \rightarrow \text{truscottite}$$

is observed between 200 and 300°C. The lower temperature limit at which this reaction proceeds is unknown.

The presence of a form of calcium sulfate in the cement, be it as an expansive agent, a set controller, or grinding aid, will always release sulfate to the groundwater up to a

limit as yet undetermined, depending on phase solubility and reaction kinetics. Reducing the amount of sulfate present in the formulation, and consequently reducing the amount of the expansive phase, ettringite, that would be formed during curing, would reduce the total sulfate that would be released from the seal but probably would not reduce its concentration in solution while it was being released.

The levels of silica present in the rocking-autoclave solutions at 150°C are lower than the concentrations from tuff of the Topopah Spring Member reported by Oversby (1984), suggesting that they are not controlled by cristobalite but by quartz or a hydrous calcium silicate such as tobermorite. At 200°C the solutions are undersaturated with respect to quartz.

REFERENCES

D. Broxton, D. Vaniman, F. Caporuscio, B. Arney, and G. Heiken, "Detailed Petrographic Descriptions and Micrograph Data for Drill Holes USW-G2 and UE25b-lH, Yucca Mountain, Nevada," Los Alamos National Laboratory report LA-9324-MS (October 1982).

S. Diamond, J. L. White, and W. L. Dolch, "Effects of Isomorphous Substitution in Hydrothermally-Synthesized Tobermorite," Am. Mineral. **51**, 388-401 (1966).

G. L. Kalousek, "Crystal Chemistry of Hydrous Calcium Silicates: I, Substitution of Aluminum in Lattice of Tobermorite," J. Am. Ceram. Soc. **40**, 74-80 (1957).

S. Komarneni, D. M. Roy, and R. Roy, "Al-Substituted Tobermorite: Shows Cation Exchange," Cem. Concr. Res. **12**, 773-780 (1982).

S. Komarneni and D. M. Roy, "Hydrothermal Interactions of Cement or Mortar with Zeolites or Montmorillonites," in Scientific Basis for Nuclear Waste Management, VI, Materials Research Society, Symposium Proceedings, Vol. 15, Douglas G. Brookins, Ed. (North-Holland, New York, 1983a), pp. 55-62.

S. Komarneni and D. M. Roy, "Tobermorites: A New Family of Cation Exchangers," Science **221**, 647-648 (1983b).

V. M. Oversby, "Reaction of the Topopah Spring Tuff with J-13 Water at 120°C," Lawrence Livermore National Laboratory report UCRL-53574 (July 1984).

D. M. Roy and A. M. Johnson, "Investigations of Stabilities of Calcium Silicate Hydrates at Elevated Temperatures and Pressures," in *Proceedings of Conference on Calcium Silicate Building Products*, S.C.I. Special Publication (Society of Chemical Industry, London, 1965), pp. 114-121.

D. M. Roy, P. H. Licastro, B. E. Scheetz,, and J. A. Fernandez, "Mechanical Compatibility Between Selected Cementitious Material and Topopah Spring Member Tuff," Sandia National Laboratory report SAND86-0558 (in preparation).

B. E. Scheetz and D. M. Roy, "Reactivity of a Tuff-Bearing Concrete: CL-40 CON-14," Los Alamos National Laboratory report (in preparation).

B. E. Scheetz, D. W. Strickler, M. W. Grutzeck, and D. M. Roy, "Physical and Chemical Behavior of Selectively Etched Fly Ashes," in Proceedings, Symposium N, Effects of Fly Ash Incorporation in Cement and Concrete, 1981, S. Diamond, Ed. (Materials Research Society, Secretariat, 110 Materials Research Laboratory, University Park, PA 16802, 1982), pp. 24-33.

H. F. W. Taylor, Ed., *The Chemistry of Cements* (Academic Press, New York, 1964).

APPENDIX A

SOLUTION ANALYSES OF AQUEOUS LIQUIDS RECOVERED AFTER REACTION OF 82-22 CONCRETE DISCS EXPOSED TO CONDENSING VAPOR OVER J-13 GROUNDWATER AT 90, 150, AND 200°C

TABLE A-I
SOLUTION ANALYSES (mmoles/ℓ) OF AQUEOUS LIQUIDS RECOVERED AFTER REACTION OF 82-22 CONCRETE DISCS EXPOSED TO CONDENSING VAPOR OVER J-13 GROUNDWATER AT 90°C

	2 months	3 months	4 months
Al_2O_3	0.019	0.019	0.019
B_2O_3	–	0.352	0.454
CaO	0.348	0.240	0.258
Fe_2O_3	–	0.009	–
K_2O	1.152	0.960	0.960
MgO	0.013	0.079	0.013
MnO	–	–	–
Na_2O	0.288	0.251	0.270
SiO_2	2.856	2.678	3.035
TiO_2	–	–	–
F	–	0.216	0.263
NO_3	0.788	0.251	0.270
SO_4	1.900	1.050	1.000
pH	10.09	9.71	9.9

TABLE A-II

SOLUTION ANALYSES (mmoles/ℓ) OF AQUEOUS LIQUIDS RECOVERED AFTER REACTION OF 82-22 CONCRETE DISCS EXPOSED TO CONDENSING VAPOR OVER J-13 GROUNDWATER AT 150°C

	2 months	3 months	4 months
Al_2O_3	0.009	0.013	0.06
B_2O_3	–	0.023	–
CaO	0.75	0.825	0.825
Fe_2O_3	–	–	0.003
K_2O	2.048	1.600	1.600
MgO	0.001	0.096	0.008
MnO	–	–	–
Na_2O	2.427	2.954	2.321
SiO_2	5.5	3.2	3.4
F	–	0.170	0.106
NO_3	0.272	0.194	0.178
SO_4	1.321	1.142	1.214
CO_3	0.139	0.026	0.035
pH	–	10.83	–

TABLE A-III

SOLUTION ANALYSES (mmoles/ℓ) OF AQUEOUS LIQUIDS RECOVERED AFTER REACTION OF 82-22 CONCRETE DISCS EXPOSED TO CONDENSING VAPOR OVER J-13 GROUNDWATER AT 200°C

	2 months	3 months	4 months
Al_2O_3	0.011	0.004	0.01
CaO	0.457	0.580	0.189
Fe_2O_3	0.001	–	–
K_2O	0.177	0.159	0.246
MgO	0.007	0.020	0.005
MnO	–	–	–
Na_2O	1.435	1.739	2.043
SiO_2	0.965	0.244	0.339
F	–	–	–
NO_3	0.145	0.081	0.081
pH	9.00	–	–

APPENDIX B

SOLUTION ANALYSES FOR VARIOUS CATIONS AND ANIONS IN AQUEOUS SOLUTION IN CONTACT WITH 82-22 CONCRETE DISCS, AT 90, 150, 200, AND 300°C

TABLE B-I

SOLUTION ANALYSES (mmoles/ℓ) FOR VARIOUS CATIONS AND ANIONS IN AQUEOUS SOLUTION IN CONTACT WITH 82-22 CONCRETE DISCS AT 90°C

	2 months	3 months	4 months
Al_2O_3	0.044	0.006	0.004
CaO	0.155	0.172	0.181
Fe_2O_3	–	0.003	–
K_2O	2.051	0.742	0.742
MgO	0.017	0.1	0.013
MnO	–	–	–
Na_2O	3.039	1.583	2.849
SiO_2	2.218	2.106	2.142
NO_3	0.161	0.140	0.150
SO_4	1.771	0.531	0.542
pH	10.04	9.91	9.90
HCO_3	1.85	–	–

TABLE B-II

SOLUTION ANALYSES (mmoles/ℓ) FOR VARIOUS CATIONS AND ANIONS IN AQUEOUS SOLUTION IN CONTACT WITH 82-22 CONCRETE DISCS AT 150°C

	T[a]	RT[b]
Al_2O_3	0.019	0.007
CaO	1.875	1.625
Fe_2O_3	–	–
K_2O	5756	2.308
MgO	0.553	0.012
MnO	–	–
Na_2O	7.813	5.425
SiO_2	2.036	0.789
NO_3	0.097	0.161
SO_4	7.604	5.938
pH	11.63	10.72

[a]Sampled at elevated temperature.

[b]Sampled at room temperature after the vessel was allowed to slowly cool.

TABLE B-III

SOLUTION ANALYSES (mmoles/ℓ) FOR VARIOUS CATIONS AND ANIONS IN AQUEOUS SOLUTION IN CONTACT WITH 82-22 CONCRETE DISCS AT 200°C

	1 month		2 months		4 months		7 months	
	T[a]	RT[b]	T	RT	T	RT	T	RT
Al_2O_3	0.215	0.011	0.278	0.019	–	0.007	–	0.007
CaO	1.4	0.9	2.375	2.0	0.15	6.5	1.25	3.5
Fe_2O_3	0.388	0.007	0.121	0.011	–	–	0.071	0.005
K_2O	1.359	1.924	1.333	0.871	0.924	0.398	1.795	0.375
MgO	0.874	–	0.200	0.037	0.083	0.021	0.125	0.12
MnO	0.011	–	0.004	–	–	–	–	–
Na_2O	3.261	3.478	5.81	6.304	12.609	7.826	7.391	7.174
SiO_2	2.321	2.50	6.083	6.534	1.723	1.585	1.723	1.862
F	0.495	0.147	0.211	0.089	–	–	–	–
NO_3	1.452	0.129	0.177	0.145	–	0.065	–	0.048
SO_4	0.938	2.083	2.5	2.917	21.875	11.875	30.208	7.5
CO_3	0.884	0.925	–	–	–	–	–	–
pH	–	–	–	–	–	–	7.5	8.3

[a]Sampled at elevated temperature.

[b]Sampled at room temperature after the vessel was allowed to slowly cool.

TABLE B-IV

SOLUTION ANALYSES (mmoles/ℓ) FOR VARIOUS CATIONS AND ANIONS IN AQUEOUS SOLUTION IN CONTACT WITH 82-22 CONCRETE DISCS AT 300°C

	1 week	2 weeks	4 weeks
Al_2O_3	0.052	0.048	0.041
CaO	3.625	4.0	3.75
Fe_2O_3	0.003	0.033	0.015
K_2O	0.177	0.277	0.433
MgO	0.08	0.025	0.025
MnO	–	–	–
Na_2O	1.435	2.214	2.565
SiO_2	9.64	5.893	3.214
TiO_2	–	–	–
F	–	–	–
NO_3	0.225	–	–
SO_4	0.526	5.521	5.313
pH	7.14	7.6	7.6

☆U.S. GOVERNMENT PRINTING OFFICE: 1989-673-034/00110

DO NOT MICROFILM COVER

Printed in the United States of America
Available from
National Technical Information Service
US Department of Commerce
5285 Port Royal Road
Springfield, VA 22161

Microfiche (A01)

Page Range	NTIS Price Code	Page Range	NTIS Price Code	Page Range	NTIS Price Code	Page Range	NTIS Price Code
001-025	A02	151-175	A08	301-325	A14	451-475	A20
026-050	A03	176-200	A09	326-350	A15	476-500	A21
051-075	A04	201-225	A10	351-375	A16	501-525	A22
076-100	A05	226-250	A11	376-400	A17	526-550	A23
101-125	A06	251-275	A12	401-425	A18	551-575	A24
126-150	A07	276-300	A13	426-450	A19	576-600	A25
						601-up*	A99

*Contact NTIS for a price quote.

DO NOT MICROFILM
COVER

Los Alamos National Laboratory
Los Alamos, New Mexico 87545